Clay Minerals (2026), 1–24
doi:10.1180/clm.2026.10054

Review Article

Attapulgite-enabled multifunctional protective coatings: structure, functionalization and applications

Qiaozhi Miao[1,2], Chaoyu Zhang[2], Wenbo Wang[2], Yue Yin[1,2] and Mei Wu[1]

[1]Huaiyin Institute of Technology, China and [2]Inner Mongolia University, Hohhot, China

Abstract

Multifunctional coatings represent the most widely used strategy for extending the service life of metallic materials in harsh environments. However, coating performance is determined by the designed functional fillers, or the micro/nano-containers. Attapulgite (ATP) has attracted increasing attention in multifunctional coating systems because it can simultaneously improve barrier performance, act as a micro/nano-container for active agents, form surface micro- and nanostructures and regulate interfacial properties. These features enable its broad use in superhydrophobic, anti-corrosion, anti-bacterial/anti-fouling, self-cleaning/anti-smudge and anti-icing coatings. This review provides a comprehensive overview of recent progress in ATP-based multifunctional protective coatings. It examines the main pretreatment strategies for ATP, including thermal treatment, acid/alkali activation, hydrothermal treatment and solvothermal treatment, together with their influence on channel characteristics, surface activity, dispersibility and matrix compatibility. The diverse roles of ATP in coating systems are further discussed, ranging from barrier-phase reinforcement and micro/nano-container construction to roughness generation and interfacial functional regulation, as well as the corresponding protective mechanisms. By integrating the discussion of passive barrier enhancement and active functional protection, this review offers a unified perspective on the design of ATP-based multifunctional coatings. In addition, current challenges and future research directions are briefly outlined to promote the practical development of high-performance ATP-enabled protective coatings.

Keywords: Attapulgite; functional fillers; micro/nano-container; modification; multifunctional coating

(Received 29 March 2026 UTC; revised 7 June 2026 UTC; accepted 3 July 2026 UTC)

The increasing complexity of service environments for metallic materials – coupled with rising demands from aerospace, marine engineering, transportation, medical devices and civil infrastructure industries for surface-protecting materials that offer integrated functionality, long-term durability and environmental compatibility – has spurred extensive research interest in high-performance multifunctional coatings (Montemor, 2014; Li *et al.*, 2015; Xavier, 2023; Qian *et al.*, 2025). Conventional protective coatings, typically designed for a single function, suffer from inherent limitations in corrosion resistance, superhydrophobicity, self-cleaning/anti-smudge performance, anti-icing capability, anti-bacterial/anti-fouling activity, environmental adaptability, damage responsiveness and multifunctional synergy. These shortcomings render them increasingly inadequate for long-term service under complex operating conditions (Lv *et al.*, 2014; Wei *et al.*, 2015; Best & Gelling, 2023; He *et al.*, 2025). Consequently, the development of multifunctional coatings capable of simultaneously integrating anti-corrosion/self-healing, superhydrophobicity, self-cleaning, anti-icing and anti-bacterial/anti-fouling properties – alongside the evolution of surface engineering strategies from single-function protection towards synergistic and adaptive protection – has emerged as a critical research frontier.

Functional protective coatings are typically designed using organic matrices integrated with functional fillers, and their performance enhancement largely depends on the structural characteristics, surface chemistry and interfacial interactions of the incorporated nanofillers (Cao *et al.*, 2009; Farhadi *et al.*, 2011; Chang *et al.*, 2013; Navarchian *et al.*, 2014; Zhou *et al.*, 2022; Zhang *et al.*, 2025a; Wang *et al.*, 2026). Among various candidate fillers (e.g. two-dimensional materials, metal oxides, silica and micro/nano-containers), attapulgite (ATP) – a naturally occurring one-dimensional fibrous hydrated magnesium aluminosilicate nanoclay – has demonstrated considerable promise for multifunctional coating applications owing to its unique crystal structure, abundant surface active sites and environmental compatibility (Belaroui *et al.*, 2014). ATP possesses a typical 2:1 layered-chain structure and rod-like crystal morphology (Wang & Wang, 2016; Ding *et al.*, 2019), with continuous nanochannels distributed along the fibre axis (Zhang *et al.*, 2018b), as well as a relatively high specific surface area (SSA), porosity and surface reactivity (Murray, 2000; Suárez & García-Romero, 2011; García-Rivas *et al.*, 2017; Galán, 1996; Zhang *et al.*, 2018c). These structural features endow ATP with multiple roles in coating systems (Liu *et al.*, 2018b; Feng *et al.*, 2022; Wu *et al.*, 2023b; Li *et al.*, 2025). First, when well dispersed and effectively integrated with the matrix, ATP increases the diffusion pathway for corrosive species penetrating

Corresponding author: Mei Wu; Email: meiwu@hyit.edu.cn

Cite this article: Miao Q, Zhang C, Wang W, Yin Y and Wu M (2026) Attapulgite-enabled multifunctional protective coatings: structure, functionalization and applications. *Clay Minerals*, 1–24. https://doi.org/10.1180/clm.2026.10054

© The Author(s), 2026. Published by Cambridge University Press on behalf of The Mineralogical Society of the United Kingdom and Ireland.

the coating, thereby enhancing barrier performance. Moreover, the abundant silanol groups on the ATP surface provide a basis for grafting, surface wettability regulation and interfacial compatibility optimization (Liu *et al.*, 2024; Yang *et al.*, 2024). Such modifications can impart superhydrophobicity, anti-icing and self-cleaning/anti-smudge functions to the coating. Second, its channel structure can serve as a micro/nano-container for active agents (e.g. corrosion inhibitors, anti-bacterial agents and low-surface-energy components), enabling the coating to achieve anti-bacterial/anti-fouling and self-healing functions. Owing to these characteristics, ATP can function not only as a reinforcing and barrier filler, but also as a micro/nano-container for storing active agents, offering the potential to integrate corrosion resistance, superhydrophobicity, self-cleaning/anti-smudge, anti-icing and anti-bacterial/anti-fouling properties (Dong *et al.*, 2018; Wang *et al.*, 2024).

Over the past decade, the research paradigm for ATP in coating systems has undergone a marked transition. Early studies primarily employed ATP as a filler to improve the mechanical properties and density of organic coatings (Lu *et al.*, 2005; Wang *et al.*, 2013b). Subsequently, with a deeper understanding of its channel structure and surface activity, ATP was increasingly used as a micro/nano-container for active agents, enabling controlled release and self-healing protection under external triggers (Ali *et al.*, 2026). Furthermore, its one-dimensional nanorod morphology has been exploited to construct anti-bacterial/anti-fouling surfaces with contact-killing effects or to serve as a loading micro/nano-container for anti-bacterial agents, thereby meeting the design requirements of green anti-bacterial systems with minimal chemical release (Jiang *et al.*, 2024). More recently, by virtue of its one-dimensional architecture and assembly capability, ATP has been widely employed to construct micro/nano-hierarchical rough structures, imparting coatings with surface functionalities such as active corrosion protection, superhydrophobicity, self-cleaning/anti-smudge, anti-icing and anti-bacterial/anti-fouling performance (Xie *et al.*, 2022). This evolution indicates that ATP has progressively transitioned from a conventional inert filler to a multifunctional filler capable of participating in interfacial regulation, active species loading and structural construction in advanced coating systems.

Despite its attractive application potential, natural ATP is commonly associated with impurities such as metal oxides, carbonates and other silicate minerals. It also suffers from particle agglomeration, partial channel blockage and insufficient utilization of surface active sites (Wang & Wang, 2016; Suárez *et al.*, 2021). These factors directly affect its dispersibility, loading capacity and interfacial compatibility, ultimately compromising its functional performance in coating systems. Therefore, while preserving its rod-like morphology and crystal framework, the rational regulation of its microstructure, channel characteristics and surface chemistry through appropriate pretreatment strategies is crucial for achieving high-performance ATP-based applications (Wang *et al.*, 2025d). To date, a variety of pretreatment approaches have been developed for ATP (Frini-Srasra & Srasr, 2008; Tang *et al.*, 2014; Wang *et al.*, 2015a; Li *et al.*, 2017; Ding *et al.*, 2021; Zhang *et al.*, 2022). Thermal treatment promotes the removal of adsorbed water and part of the structural water, improves channel accessibility and optimizes the SSA (Frini-Srasra & Srasr, 2008). Acid treatment facilitates impurity removal, channel reopening and surface structure optimization and is frequently used to improve loading capacities (Ding *et al.*, 2021; Zhang *et al.*, 2022). Alkali treatment, in contrast, is advantageous for increasing surface activity and interfacial reactivity (Wang *et al.*, 2015a). Hydrothermal or solvothermal treatment can further regulate ATP's crystal phase, morphology and surface structure (Li *et al.*, 2017). These pretreatment and modification strategies determine not only the structural and interfacial characteristics of ATP itself, but also its mode of action and performance in multifunctional coating systems.

The preceding discussion indicates that ATP-based multifunctional coatings have made notable progress in anti-corrosion, superhydrophobicity, self-cleaning, anti-icing and anti-bacterial/anti-fouling applications (Tang *et al.*, 2014; Jing *et al.*, 2020; Li *et al.*, 2023; Qiu *et al.*, 2023; Wu *et al.*, 2023b; Wang *et al.*, 2024; Zhang *et al.*, 2024b). Nevertheless, several critical challenges remain unresolved. For instance, the loading capacity and release kinetics of ATP when used as a micro/nano-container still lack precise regulation; the long-term service stability of coatings under coupled environments involving salt spray, ultraviolet irradiation, freeze–thaw cycling and mechanical wear requires systematic evaluation; green, fluorine-free surface modification strategies and integrated approaches for constructing multiple functionalities remain to be further developed; and, importantly, the dynamic interfacial interaction mechanisms among ATP, functional molecules, coating matrices and metallic substrates have not yet been fully elucidated. These issues considerably constrain the rational design, performance optimization and large-scale application of ATP-based multifunctional coatings.

Extensive research has been reported on the development of nanoclay materials in fields such as environmental decontamination, advanced electrochemical energy conversion, corrosion protection, anti-bacterial applications and drug delivery (Yeh & Chang, 2008; Zaarei *et al.*, 2008; Zahidah *et al.*, 2017; Wang *et al.*, 2020c; Leal *et al.*, 2022; Beryl & Xavier, 2023; Wu *et al.*, 2023a; Xie *et al.*, 2023a; Biswas *et al.*, 2024; Mao *et al.*, 2024a; Naciri *et al.*, 2024; Xiang *et al.*, 2024; Zhang *et al.*, 2025c). To the best of the authors' knowledge, however, no review has been devoted to employing the same nanoclay for the construction of multifunctional coatings. Only a few reviews have summarized specific minerals for anti-corrosion coatings (Yeh & Chang, 2008; Zaarei *et al.*, 2008; Zahidah *et al.*, 2017; Leal *et al.*, 2022; Beryl & Xavier, 2023; Xiang *et al.*, 2024). Therefore, a systematic review summarizing the development of ATP-based multifunctional coatings is urgently needed. As illustrated by the publication and citation trends in Fig. 1a, ATP-based multifunctional coatings have attracted increasing research attention from 2010 to 2026. This review provides a comprehensive and detailed discussion of the application of ATP-based nanoclays in multifunctional coatings (Fig. 1b), focusing on the pretreatment of ATP and its applications in anti-corrosion, superhydrophobicity, self-cleaning/anti-smudge, anti-icing and anti-bacterial/anti-fouling coatings. Specifically, the major pretreatment strategies – including thermal treatment, acid/alkali treatment, hydrothermal treatment and solvothermal treatment – are summarized, with an emphasis on their effects on the microstructure, channel characteristics and surface chemistry of ATP. Building on this foundation, the applications and working mechanisms of ATP in five key categories of functional coatings are further discussed: (1) its dual role in anti-corrosion coatings as both a physical barrier and a stimuli-responsive micro/nano-container for corrosion inhibitors; (2) its role in constructing surface micro/nano-roughness and low-surface-energy materials in superhydrophobic coatings; (3) its excellent superhydrophobic characteristics that endow coatings with self-cleaning/anti-smudge functions; (4) its application potential in anti-icing coatings for low ice adhesion, delayed icing and synergistic de-icing in combination with photothermal components; and (5) its functional

https://doi.org/10.1180/clm.2026.10054 Published online by Cambridge University Press

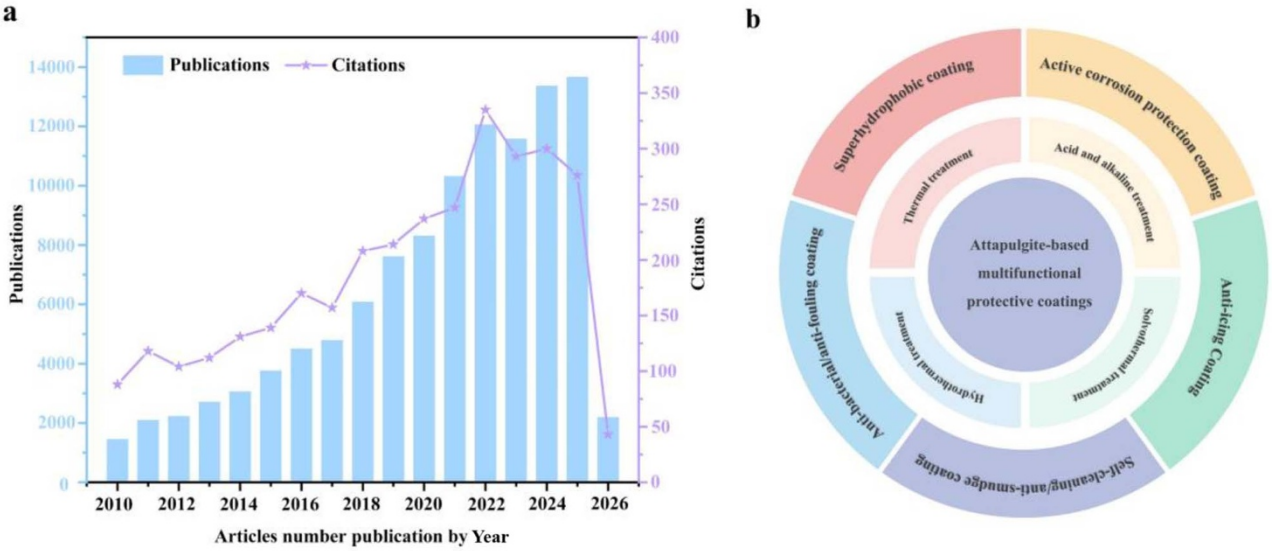


Figure 1. (a) Annual publication output and citation trends of ATP-based multifunctional protective coatings, reflecting growing research interest in this field (data sourced from the Web of Science Core Collection using the keywords 'Attapulgite' and 'Coating'). (b) Schematic illustration of the review structure, outlining the pretreatment and modification strategies of ATP and their subsequent applications in various multifunctional protective coatings, including active corrosion protection, self-cleaning/anti-smudge, anti-bacterial/anti-fouling, anti-icing and superhydrophobic coatings.

contributions to anti-bacterial/anti-fouling coatings based on its one-dimensional nanostructure and active agent-loading capability. This review aims to establish relationships between ATP pretreatment strategies and coating structural design, interfacial regulation and ultimate functional performance, thereby providing valuable guidance for the development of multifunctional, environmentally friendly and application-orientated ATP-based coatings.

Pretreatment of ATP

Due to their natural formation and paragenetic processes, ATP deposits typically contain coexisting mineral impurities, including metal oxides, carbonates and silicates. As a result, raw ATP often exhibits a broad particle-size distribution, severe agglomeration, partial pore blockage and a low density of surface active sites. These inherent limitations severely compromise its performance as a micro/nano-container, manifesting as low loading capacity, poor dispersibility, weak interfacial compatibility and insufficient structural stability. Consequently, to meet the stringent demands of applications such as nanomedicine delivery, catalysis and functional composite systems, ATP generally requires systematic pretreatment or activation to improve its SSA.

To date, thermal activation, acid/alkali treatment, hydrothermal treatment and solvothermal treatment have been widely adopted for the targeted modulation of ATP. The goal of these pretreatment strategies is to achieve an optimized 'purification–structural regulation–surface functionalization' cascade while preserving ATP's characteristic rod-like morphology and crystalline framework. Specifically, pretreatment improves ATP in the following aspects. First, it improves SSA and pore volume. By removing mineral impurities and volatile components, the internal pore network is reopened, leading to increased SSA and pore volume, which in turn boosts ATP's capacity for high loading capacity. And second, it improves dispersion and active site availability. Precise control over the degree of dehydroxylation, ion-exchange capacity and the density and charge characteristics of surface hydroxyl groups not only improves dispersion stability in solvents or polymer matrices but also strengthens interfacial interactions with active agents or functional components, thereby providing abundant reactive sites for subsequent grafting, adsorption or immobilization. In this section, we discuss how these strategies modulate ATP's microstructure, pore architecture and surface chemistry, with the goal being to establish a robust material foundation for ATP in high-performance coating applications.

Thermal treatment

Thermal treatment is a straightforward and cost-effective modification strategy for ATP, enabling control of its structural features and surface properties by selectively removing physically adsorbed water, structurally bound water and volatile organic contaminants (Biswas *et al.*, 2016; Cai *et al.*, 2025). In practical applications, precise control of the thermal profile is critical for achieving the desired microstructure and surface chemistry, as excessive temperature and/or prolonged duration may trigger pore collapse, loss of the crystalline framework or undesirable phase transformations. Generally, water in ATP is classified into three states (Bradley, 1940): (1) surface/interparticle adsorbed water together with zeolitic water residing in the channel system; (2) coordinated water associated with Mg/Al coordination; and (3) structural hydroxyls/water located within the octahedral sheet (VanScoyoc *et al.*, 1979; Frini-Srasra & Srasr, 2008). Although the characteristic dehydration temperatures may vary slightly among ATP sources due to differences in composition and morphology, the overall dehydration pathway remains qualitatively similar. The chemical composition of ATP varies significantly depending on its geological location, which in turn influences its thermal behaviour, structural stability and surface properties. Table 1 summarizes chemical composition data for representative ATPs from various geographical regions reported in the literature (Bradley, 1940; Belaroui *et al.*, 2014; Zhang *et al.*, 2015a; Ding *et al.*, 2019; Zhuang *et al.*, 2022).

Thermal treatment significantly influences the morphology, phase composition and pore characteristics of ATP.

https://doi.org/10.1180/clm.2026.10054 Published online by Cambridge University Press

Table 1. Chemical compositions (wt.%) of ATPs from various locations.

Location	SiO_2	Al_2O_3	MgO	Fe_2O_3	CaO	Na_2O	K_2O	Others	Reference
China (Anhui)	51.47	9.65	10.78	4.95	0.69	0.009	0.96	–	Zhang *et al.* (2015a)
Algeria	40.32	8.87	8.88	3.27	9.69	0.21	0.89	–	Belaroui *et al.* (2014)
China (Gansu)	56.54	14.52	5.34	7.42	4.59	0.15	3.72	–	Ding *et al.* (2019)
USA (Georgia)	55.03	10.24	10.49	3.53	n.d.	n.d.	0.47	–	Bradley (1940)
China (Jiangsu)	63.11	11.94	13.61	6.32	2.10	0.24	1.32	1.36	Zhuang *et al.* (2022)

n.d. = not determined.

Thermogravimetric analysis (TGA) profiles of ATP obtained across a range of temperatures are presented in Fig. 2a, elucidating the progressive structural evolution during thermal treatment as evidenced by distinct stages of mass loss and corresponding variations in thermal stability. Specifically, below 120°C, the removal of adsorbed water predominates and proceeds without discernible alteration of the crystal structure. In the range of 120–150 °C, desorption of a small amount of zeolitic water occurs, accompanied by a slight modification of the crystal structure (Kuang *et al.*, 2004). In the 150–280°C range, most channel-hosted zeolitic water is removed; the unit-cell volume contracts while the framework is largely preserved, channel accessibility increases and the SSA correspondingly increases (Post & Heaney, 2008; Cheng *et al.*, 2011; Boudriche *et al.*, 2012). At 340–480°C, coordinated water begins to be eliminated, potentially inducing structural folding; as the temperature approaches ∼450°C, this folding tends to become irreversible, causing damage to the periodic structure, collapse of the channel network and a rapid decrease in SSA (Kuang *et al.*, 2004; Liu *et al.*, 2013). At higher temperatures (500–700°C), dehydroxylation and decomposition of impurities become predominant, and the ATP progressively becomes amorphous. Above 800°C, pronounced phase transformations may occur, such as the formation of cristobalite. The phase composition as a function of thermal treatment temperature is shown in Fig. 2b. With increasing temperature, the intensities of the diffraction peaks at 8.3°2θ, 19.8°2θ, 21.4°2θ and 27.5°2θ gradually decrease. In addition, new diffraction peaks at 9.6°2θ and 18.8°2θ emerge, corresponding to the structural rearrangement of the (110) and (040) planes. At higher temperatures, the interplanar spacing of the (130) plane decreases due to the loss of coordinated water within the pore structure of ATP.

These structural changes significantly affect the surface properties of ATP. As shown in Fig. 2c, the SSA and pore volume are governed by the evolution of the crystalline framework and the removal of internal water/volatile matter. With increasing temperature, the SSA initially increases and then decreases. The enhancement observed for ATP-180 is ascribed to the loss of zeolitic water (Zhuang *et al.*, 2022). Upon removal of coordinated water, ATP-300 begins to undergo structural rearrangement. In contrast, ATP-570 exhibits a pronounced decrease in SSA and pore volume due to the loss of structural and coordinated water, accompanied by concomitant channel collapse. These samples originate from Jiangsu, China, with their chemical compositions detailed in Table 1, and the suffix numbers denote their respective thermal treatment temperatures (180°C, 300°C and 570°C).

The dehydration of ATP with increasing temperature is accompanied by pronounced morphological changes, as shown in Fig. 2d–f. At 200°C (Fig. 2d), ATP retains its typical fibrous morphology, composed of well-defined rod-like nanostructures with relatively smooth surfaces and clear boundaries. At 1000°C (Fig. 2e), the fibrous structure is still largely preserved, although slight aggregation and local structural distortion can be observed. At ∼1100°C, significant melting of the ATP fibres is observed (Fig. 2f), leading to their fusion into a dense, interwoven network structure (Wang *et al.*, 2020b). The structural evolution of ATP during thermal treatment is schematically illustrated in Fig. 2g (Zhuang *et al.*, 2022). Water species (adsorbed, zeolitic and coordinated) distributed within the one-dimensional channels govern structural stability. Their sequential removal upon heating induces progressive framework rearrangement and contraction, ultimately resulting in channel collapse.

These discussion demonstrates that thermal treatment is an effective strategy to enhance SSA, optimize microstructure and regulate the phase composition of ATP through the removal of physically and chemically bound water, the opening of pore channels and the activation of surface hydroxyl groups. These changes significantly improve the reactivity and functional performance of ATP. Nevertheless, thermal treatment has inherent limitations. Excessive heating may induce structural collapse, loss of crystallinity and undesirable phase transformations, thereby deteriorating the properties of ATP. A key challenge lies in precisely controlling the treatment parameters (e.g. temperature, duration and atmosphere) to achieve an optimal balance between structural activation and preservation. Future research should focus on several aspects. First, integrating thermal treatment with other modification strategies, such as molten salt-assisted methods, may reduce the required temperature while preserving the structural integrity of ATP. Second, the development of advanced *in situ* characterization techniques is essential for real-time monitoring of structural evolution during thermal treatment, which would enable a deeper understanding of the transformation mechanisms. Establishing a clear correlation between thermal treatment conditions and the evolution of ATP properties is crucial for customizing ATP-based functional materials. Ultimately, precise control of processing parameters enables the rational design of ATP with tailored properties for high-performance applications while promoting the development of energy-efficient and scalable modification processes.

Acid and alkaline treatment

Acid and alkaline treatment effectively remove impurities (e.g. carbonates, sulfates and metal oxides) from ATP, open its intrinsic channel structures and significantly increase both its SSA and pore volume (Zhang *et al.*, 2010; Boudriche *et al.*, 2011; España *et al.*, 2019). This treatment typically involves dispersing ATP in aqueous solutions of inorganic acids (e.g. HCl, H_2SO_4, HNO_3 or H_3PO_4) to obtain the desired product by adjusting critical parameters, including acid concentration, reaction duration and temperature (Barrios *et al.*, 1995; Ye *et al.*, 2006; Cai *et al.*, 2007; Shawabkeh *et al.*, 2007; Volzone, 2007; Zhang *et al.*, 2010). The acid treatment mechanism involves the progressive dissolution of the octahedral sheets of ATP, which removes interlayer metal cations. Residual

https://doi.org/10.1180/clm.2026.10054 Published online by Cambridge University Press

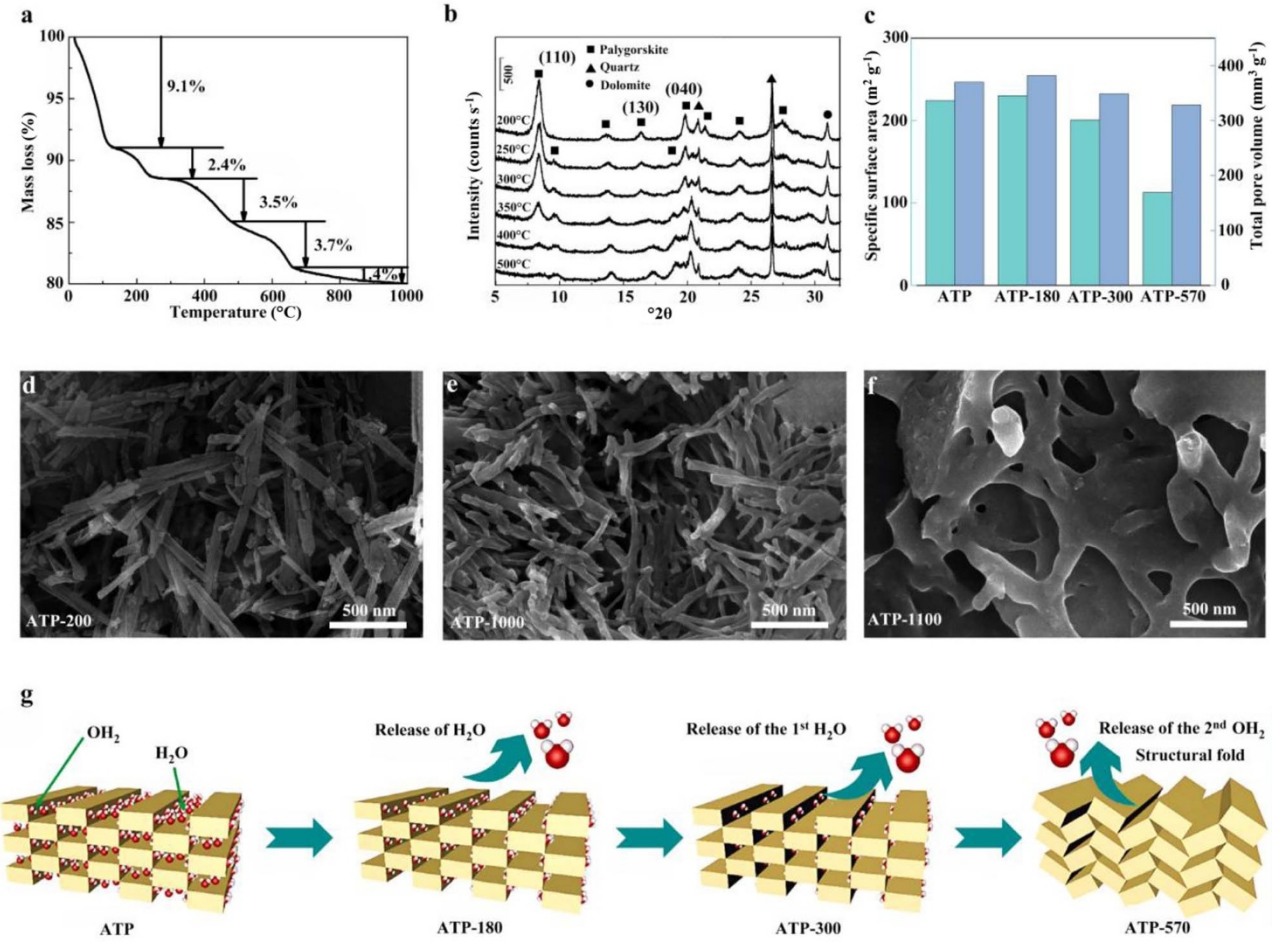


Figure 2. (a) Representative TGA profile of ATP. (b) X-ray diffraction trace of ATP subjected to thermal pretreatment at various temperatures (Liu *et al*., 2013). (c) SSA and pore volume of ATP as a function of temperature (Zhuang *et al*., 2022). (d–f) Scanning electron microscopy images of ATP at various temperatures: (d) 200°C, (e) 1000°C and (f) 1100°C (Wang *et al*., 2020b). (g) Schematic illustration of the structural evolution of water molecules and channels in ATP (Zhuang *et al*., 2022).

octahedral fragments continue to support the tetrahedral sheets, thereby preserving the fundamental fibrous chain-layer framework (Gonzalez *et al*., 1989; Frini & Srasra, 2010). This structural evolution alters the surface properties of ATP: the leaching of metal cations cleaves some Si–O–*M* bonds, generating deprotonated Si–O$^-$ sites, which are subsequently protonated to form silanol groups under sustained acidic conditions. This process can significantly modify the surface properties of ATP and increase its SSA and porosity, increasing its potential as a micro/nano-container for active agents in the fields of corrosion protection and drug delivery (Ding *et al*., 2019).

Numerous previous studies have reported the use of acid treatment strategies to improve crystal bundle disintegration, compositional optimization and pore architecture (Myriam *et al*., 1998; Guan *et al*., 2018). The present work mainly focuses on optimizing acid concentration and type to establish preparation parameters that correlate with ATP structure. For example, HCl treatment has been widely used to tailor the structure and properties of ATP. As shown in Fig. 3a, acid treatment can transform ATP into micro/nano-containers suitable for storing active agents (Li *et al*., 2025). As illustrated in Fig. 3b, HCl treatment effectively removes interlayer metal cations and carbonate impurities from the octahedral sheets, leading to compositional purification and structural modification. By optimizing the HCl concentration, the SSA and pore volume increase from 74 $m^2\ g^{-1}$ and 0.21 $cm^3\ g^{-1}$ for pristine ATP to 351 $m^2\ g^{-1}$ and 0.77 $cm^3\ g^{-1}$ for acid-etched ATP, enabling a high active agent-loading capacity (Fig. 3c). Moreover, electrostatic repulsion between rod-like crystals is increased, promoting bundle dissociation and improving dispersibility (Fig. 3d). Further research has systematically investigated the effects of acid concentration and reaction duration on the SSA of ATP (Yeh *et al*., 2013). The results revealed that excessive acidity or prolonged treatment induces physical degradation of ATP (e.g. thinning and shortening), loss of characteristic channel structures and even transformation towards amorphous silica, ultimately diminishing SSA (Fig. 3e). Acid type is another important parameter in determining the characteristics of ATP. One study compared the effects of HCl and H_3PO_4 treatments on ATP porosity, finding that HCl treatment preferentially expands meso/macro-pores, whereas H_3PO_4 treatment prompts micropore formation. Therefore, acid concentration and type play a crucial role in controlling the SSA and morphology of ATP. An optimal balance must be achieved between the moderate extraction of Mg, Al and other cations from octahedral sheets to unblock channels and improve micro/nano-container functionality and the prevention of excessive etching that compromises structural integrity. This strategic equilibrium ensures the

https://doi.org/10.1180/clm.2026.10054 Published online by Cambridge University Press

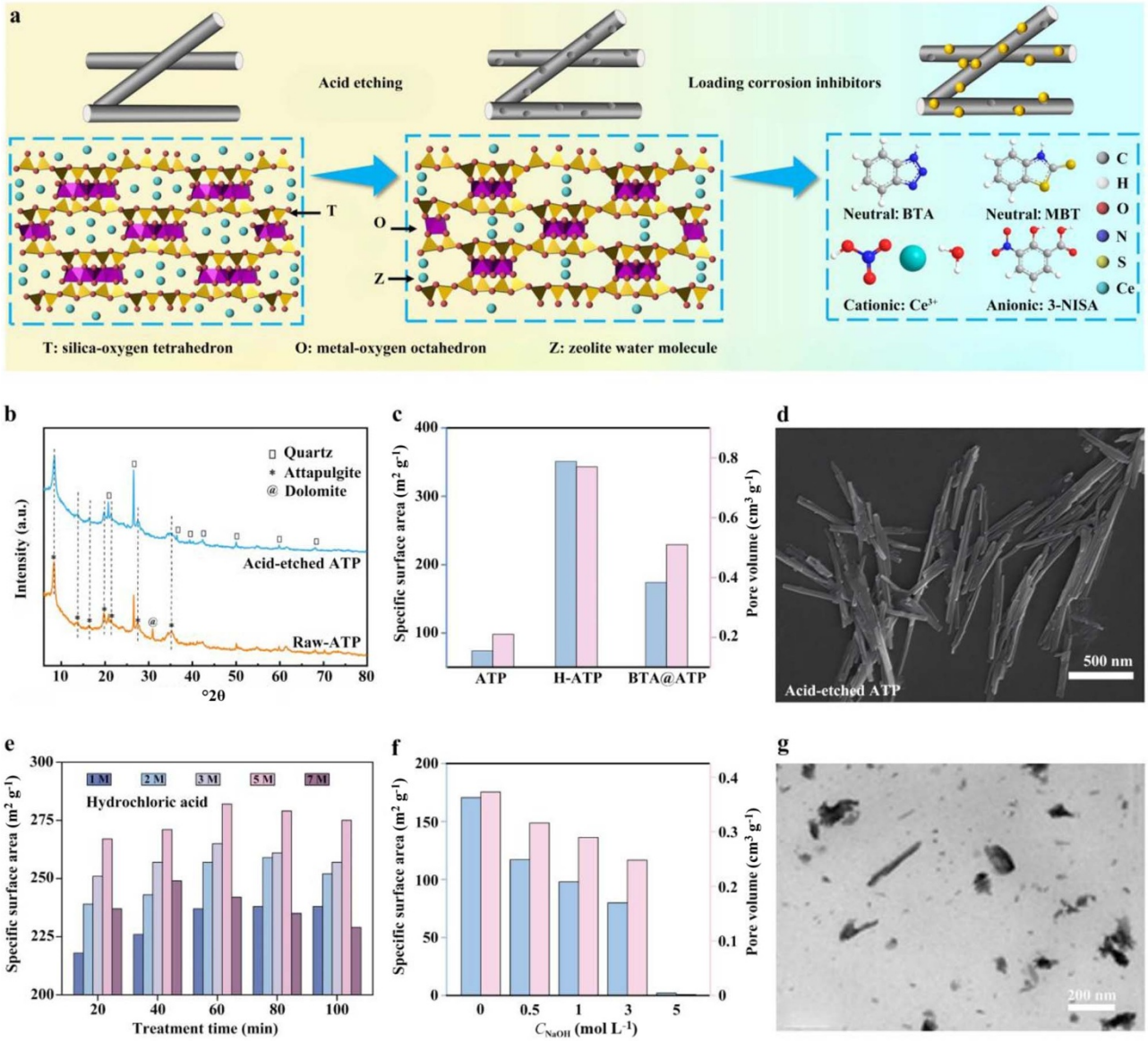


Figure 3. (a) Schematic illustration of the preparation of inhibitor@ATP containers. (b) X-ray diffraction traces of pristine ATP and acid-etched ATP. (c) SSA and pore volume of pristine ATP, acid-etched ATP and benzotriazole (BTA)@ATP. (d) Scanning electron microscopy image of acid-etched ATP (Li *et al.*, 2025). (e) Time-dependent evolution of SSA for ATP etched with various HCl concentrations (Yeh *et al.*, 2013). (f) Effect of NaOH concentration on the SSA and pore volume of ATP. (g) Transmission electron microscope image of ATP after pretreatment with 5 M NaOH (Wang *et al.*, 2015a). 3-NISA = 3-nitrosalicylic acid; MBT = 2-mercaptobenzothiazole.

preservation of the fibrous framework while maximizing ATP's efficacy as a functional micro/nano-container.

Alkaline treatment of ATP exhibits distinct selectivity: under strongly alkaline conditions, cations such as Al^{3+} and Mg^{2+} within the octahedral sheets are progressively leached, concurrently inducing localized degradation and rearrangement of the Si–O tetrahedral framework. This selectivity is typically evidenced by a higher dissolution extent of Si^{4+} relative to Al^{3+} and Mg^{2+}, with Al^{3+} leaching more readily than Mg^{2+} – a behaviour closely correlated with the spatial distribution of bond dissociation energies (Wang *et al.*, 2015a; Lu & Wang, 2022). Alkaline treatment uniquely facilitates surface charge modulation and controlled structural evolution, substantially increasing the density of surface hydroxylation and thereby enhancing interfacial reactivity and functionalization potential for subsequent modifications (e.g. silanization and grafting; Wang *et al.*, 2013a; He & Jin, 2023; Lisuzzo *et al.*, 2023). Previous studies have shown that the SSA of ATP decreases progressively with increasing NaOH concentration (Fig. 3f; Wang *et al.*, 2015a). Further structural analysis reveals that alkaline treatment exerts a concentration-dependent regulation on the structural evolution of ATP. The process proceeds *via* a controllable selective dissolution mechanism. Hydroxide ions preferentially attack the Si–O–Si and Si–O–*M* (*M* = Mg, Al) bonds, leading to framework cleavage and the formation of Si–O^{-}. At relatively low to moderate NaOH concentrations (≤3.0 mol L^{-1}), selective leaching of octahedral cations (e.g. Al^{3+} and Mg^{2+}) occurs, resulting in only slight structural modification, while the fibrous morphology and the tetrahedral–octahedral framework remain largely preserved. In contrast, when the NaOH concentration increases to 5.0 mol L^{-1}, extensive dissolution of Al, Mg and Si

https://doi.org/10.1180/clm.2026.10054 Published online by Cambridge University Press

species from the crystal backbone occurs, leading to the destruction of the ribbon-layer structure and the eventual collapse of the pore system, as evidenced by morphological changes (Fig. 3g).

Acid and alkaline treatments provide effective routes for tuning the structure and surface properties of ATP. Acid treatment generally increases SSA, pore volume and dispersibility by removing impurities, leaching octahedral cations and reopening blocked channels. In contrast, alkaline treatment can induce structural evolution and surface hydroxylation through the selective dissolution of framework components. These changes are beneficial for improving the reactivity, storage capacity and subsequent functionalization of ATP.

Nevertheless, both treatments require careful control of the synthesis parameters to obtain the desired products. Excessive acid treatment may result in serious damage to the octahedral sheets and even promote the formation of amorphous silica, while strong alkaline treatment may cause framework collapse and destruction of the pore structure due to extensive dissolution of both octahedral cations and tetrahedral silica. A major challenge, therefore, lies in achieving sufficient structural activation without compromising the intrinsic framework stability of ATP. Future work should focus on improving the controllability of these chemical treatment processes and elucidating their underlying mechanisms. Combining acid or alkaline treatment with other approaches, such as thermal activation or template-assisted methods, may offer more precise regulation of pore architecture and surface chemistry. Moreover, research efforts should be directed towards tracking structural evolution during dissolution and reconstruction, so that the relationship between treatment conditions and the resulting structural and functional properties can be established on a more quantitative basis. Such efforts will be essential for the rational design of ATP with optimized performance and for the development of efficient and scalable treatment processes.

Hydrothermal treatment

Hydrothermal treatment involves subjecting a material to controlled temperature and pressure within a sealed system, using water as the reaction medium to induce dissolution, recrystallization, phase transformation and morphological reconstruction. This process enables precise tuning of ATP's crystalline phase composition, pore-structure distribution and surface functional group states.

Under hydrothermal conditions, ATP can be transformed into a smectite phase. Dispersed ATP in weakly alkaline deionized water was almost completely transformed into smectite nanosheets through hydrothermal treatment (Wang *et al.*, 2015b). As shown in Fig. 4a, the characteristic ATP diffraction peaks at 8.36°2θ and 13.89°2θ gradually disappeared, while a new smectite (001) peak emerged at 6.05°2θ (Fig. 4b), confirming the transformation of ATP into smectite. Correspondingly, with extending reaction time, ATP nanorods progressively shortened and transformed into nanosheets. At 2 h (Fig. 4c), only a limited number of sheet-like structures were observed, indicating that the transformation was still at an initial stage. By 12 h (Fig. 4d), the number of nanorods had significantly decreased, while nanosheets became the dominant morphology, suggesting that the transformation had advanced substantially. At reaction times of ≥24 h (Fig. 4e), the rod-like structures were almost entirely replaced by nanosheets, ultimately resulting in the formation of smectite nanosheets. Mechanistic studies revealed that this phase transformation does not proceed *via* the conventional 'dissolution–recrystallization' pathway; rather, it occurs through the reconnection of 'polysome' structural units following the 'proximity principle'. Under alkaline conditions, the high-energy Si–O–Si bonds linking oppositely orientated Si–O tetrahedra are selectively cleaved, which promotes the alignment of tetrahedral layers. These layers then reorganize according to the 'proximity principle' under *c*/2 glide. In addition, Al^{3+} and Mg^{2+} participate in the reconstruction of the octahedral layers. Several studies (Yang *et al.*, 2010; Jiang *et al.*, 2014; Youcef *et al.*, 2020) have indicated that ATP can effectively replace expensive chemical precursors (e.g. tetraethyl orthosilicate (TEOS), colloidal silica and silicic acid) in the hydrothermal synthesis of high-value zeolites and ordered mesoporous materials. For instance, ZSM-5 zeolite (Zeolite Socony Mobil-5; Li *et al.*, 2017) was synthesized using natural ATP as a silica source *via* a vapour-induced transformation (VIT) strategy (Fig. 4f). Water vapour permeates the ATP framework, inducing rearrangement and crystallization of Si/Al species to yield ZSM-5 with high crystallinity (yield ≈ 96%) and a well-developed porous architecture, exhibiting performance comparable to counterparts synthesized from pure chemical reagents. The X-ray diffraction (XRD) trace presents the typical peaks associated with an MFI-type (Mobil Five framework-type) structure, with characteristic diffraction peaks at 7–9°2θ and 22–25°2θ, while the ATP peak (typically at 8.4°2θ) disappears (Fig. 4g). The scanning electron microscopy (SEM) image of the resulting ZSM-5 (Fig. 4h) exhibits nearly perfect coffin-shaped crystals, which are fundamentally different from the fibrous morphology of ATP. The XRD traces of zeolites synthesized from various ATP sources (Fig. 4i) present the characteristic diffraction peaks of ZSM-5, demonstrating that ATPs from different regions with varying compositions can be used as Si/Al sources for zeolite synthesis *via* the VIT method.

SBA-15 (Santa Barbara Amorphous-15) and MCM-41 (Mobil Composition of Matter No. 41), two widely used mesoporous materials, can also be synthesized from ATP. For example, Jiang *et al.* (2014) used ATP as both a template and a silica source. Acid-treated ATP was obtained through HCl-assisted hydrothermal treatment. The resulting product was then used as a hard template to construct a carbonaceous composite *via* vapour-phase polymerization of furfuryl alcohol. Subsequently, the template was removed, and the silica species were recovered through high-temperature hydrothermal alkaline treatment in NaOH solution. The recovered alkaline leachate was then mixed with an HCl solution containing Pluronic P123 (EO_{100}–PO_{70}–EO_{100}, where EO = ethylene oxide, PO = propylene oxide and subscript numbers denote the average number of repeating units in each block), followed by hydrothermal assembly and calcination to produce SBA-15. This strategy highlights the dual role of ATP under hydrothermal conditions as both a template and a silicon source for the preparation of porous materials. In a related study, Chen *et al.* (2025) further replaced TEOS with acidified ATP (PATP) to synthesize MCM-41, and they elucidated its formation mechanism (Fig. 4j). During acidification, H^+ dissolves metal ions and attacks the silicate framework, generating abundant Si–O^- groups and thereby imparting a negative surface charge to PATP. During the hydrothermal process, OH^- promotes the fragmentation of PATP rods into colloidal particles and debris. These negatively charged species then electrostatically interact with cetyltrimethylammonium ions (CTA^+), leading to the formation of PATP–CTA^+ micellar rods. These subsequently self-assemble into a regular, mesoporous, 'chrysalis-like' structure (dominated by colloidal particles) and an irregular, mesoporous, 'cotton-like' structure (reconstructed from fragments). The resulting PATP–MCM-41 retains

https://doi.org/10.1180/clm.2026.10054 Published online by Cambridge University Press

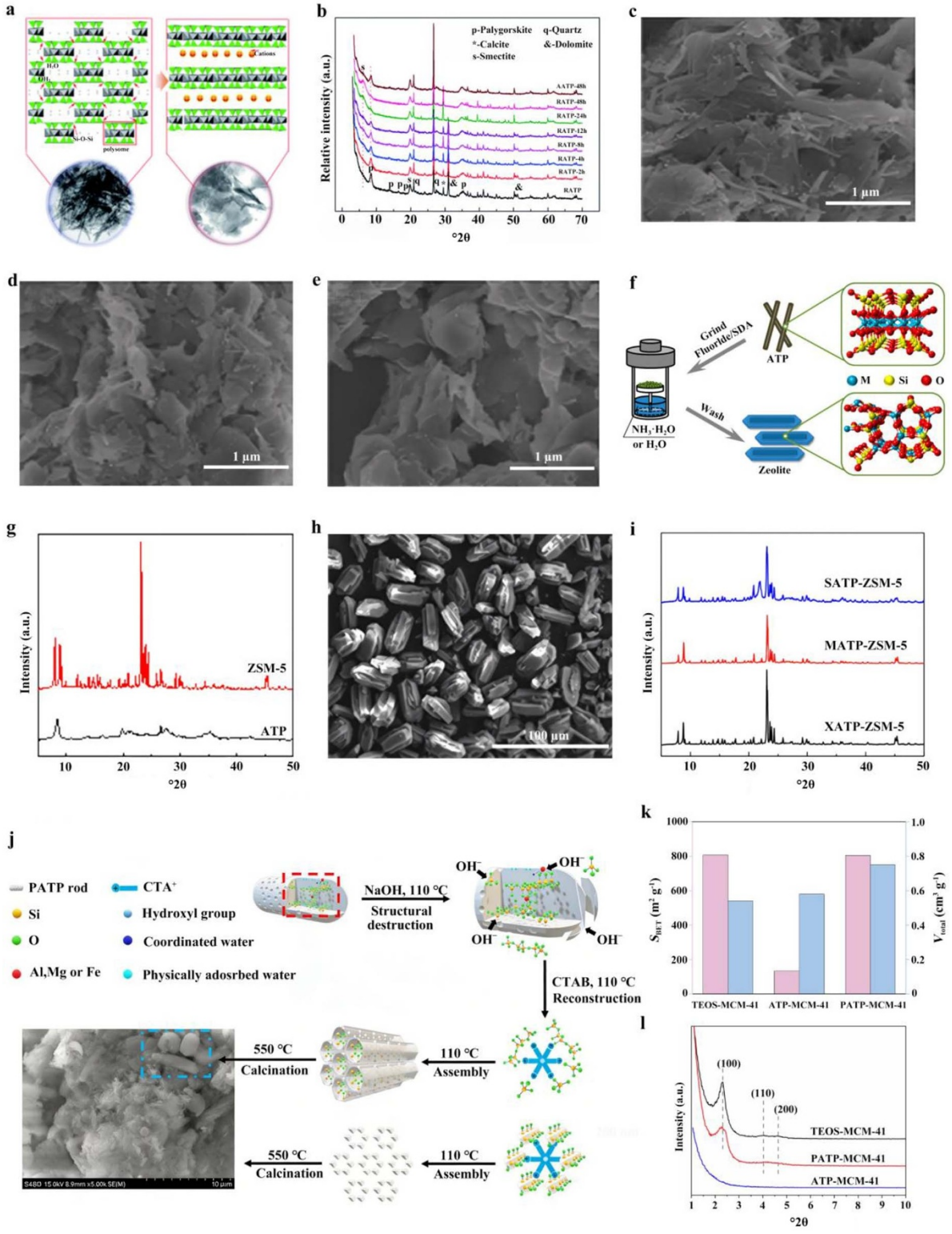


Figure 4. (a) Proposed mechanisms for the transformation from RATP (ball-milled natural ATP) nanorods to smectite nanosheets. (b) XRD traces of RATP, RATP-2h, RATP-4h, RATP-8h, RATP-12h, RATP-24h, RATP-48h and AATP-48h. (c–e) Field-emission SEM images (Wang *et al.*, 2015b) of (c) RATP-2h, (d) RATP-12h and (e) RATP-24h. (f) Scheme for the direct synthesis of zeolite from ATP *via* the VIT method. (g) XRD traces of ATP and ZSM-5. (h) SEM image of ZSM-5. (i) XRD traces of ZSM-5 from various ATP, XATP, MATP and SATP sources, denoting ATP from Xuyi, Mingguang and Shijiazhuang, China, respectively (Li *et al.*, 2017). (j) Schematic of the structural transition of PATP–MCM-41 during MCM-41 construction. (k) SSAs and pore volumes of TEOS–MCM-41, ATP–MCM-41 and PATP–MCM-41. (l) Small-angle XRD traces of TEOS–MCM-41, ATP–MCM-41 and PATP–MCM-41 (Chen *et al.*, 2025). CTAB = cetyltrimethylammonium bromide; SDA = structure-directing agent.

https://doi.org/10.1180/clm.2026.10054 Published online by Cambridge University Press

substantial Si–O^- groups. Finally, the template agent is removed by high-temperature calcination to yield the synthesized MCM-41. N_2 adsorption–desorption analysis confirms that while its SSA is comparable to that of TEOS-derived MCM-41, it possesses a larger pore volume (Fig. 4k). Moreover, PATP–MCM-41 not only exhibits canonical MCM-41 features (Fig. 4l) but also preserves the residual macroporous structures inherited from pristine ATP.

Hydrothermal treatment is an effective approach for regulating the phase composition, morphology and pore structure of ATP under controlled aqueous conditions. Through phase transformation, structural reconstruction and template-directed assembly, ATP can be converted into a variety of value-added materials, including other nanoclay minerals, zeolites and ordered mesoporous structures. These transformations greatly expand the structural tunability of ATP-derived materials and increase their potential for further functional applications. However, the outcome of hydrothermal treatment is highly sensitive to processing conditions. Inappropriate reaction parameters may lead to incomplete conversion, excessive framework dissolution, structural heterogeneity and poor pore ordering, all of which are detrimental to material performance. The key challenge, therefore, lies in directing the transformation process in a controlled manner while preserving the desired structural features. Future studies should pay greater attention to the influence of precursor characteristics on hydrothermal behaviour, particularly for ATP raw materials from various geological locations. A deeper understanding of how phase, morphology and pore structure evolve under various hydrothermal conditions will be essential for elucidating the transformation pathways. Furthermore, more informative characterization of intermediate states during treatment would help to reveal the mechanisms governing dissolution, recrystallization and structural organization. Practical aspects of hydrothermal processing – including energy consumption, reagent recycling and scalability – should also be considered. Progress in these areas will support the development of more controllable and economically viable routes for preparing ATP-derived materials with tailored structures and properties.

Solvothermal treatment

Solvothermal treatment has been widely adopted for the controlled synthesis of novel inorganic nanomaterials (Mu *et al.*, 2013b; Wang *et al.*, 2013c; Xu *et al.*, 2013a; Zhang *et al.*, 2018c; Tan *et al.*, 2021). This approach utilizes solvents (e.g. organic solvents, alcohols), thereby offering a more versatile chemical environment for regulating the structure, morphology and physicochemical properties of the nanomaterials. During solvothermal treatment, the solvent medium not only facilitates the deagglomeration and dispersion of crystalline bundles but also tailors the surface chemistry and crystal microstructure. Notably, during the solvothermal treatment of natural ATP, organic solvent molecules may engage in specific interactions with the mineral, partially substituting structural water molecules. This induces a synergistic evolution of both structure and functionality, laying the foundation for its subsequent application as a functional filler in composite materials.

The morphology, surface characteristics and pore structure of ATP can be modulated by optimizing the solvent during the solvothermal treatment process. One study (Xu *et al.*, 2013b) systematically investigated the influence of various solvent media – namely water, methanol (MT), ethanol (ET), isopropanol (IPA), dimethylformamide (DMF) and dimethyl sulfoxide (DMSO) – in combination with high-pressure homogenization on the dispersibility of ATP. Compared to the large-sized bundles of pristine ATP (Fig. 5a), DMSO-treated ATP exhibited effectively promoted deagglomeration, yielding highly dispersed, individual rod-like crystals (Fig. 5b). The results demonstrated that solvent molecules can intercalate into the pore channels of ATP, leading to host–guest interactions, while simultaneously improving the SSA and pore volume (Fig. 5c). In contrast, the isopropanol-treated system imparted optimal colloidal stability to the suspension, achieving a viscosity as high as 2364 mPa·s. This study highlights the critical roles of solvent parameters (e.g. vapour pressure, viscosity and surface tension) in regulating the dispersion behaviour of ATP, providing a processing foundation for obtaining highly dispersed ATP without the need for the surfactants or high-temperature treatments typically required in conventional strategies.

Further work investigated the effects of solvothermal treatment on the structure and surface properties of natural ATP using solvents of various polarities, including methanol, ET, IPA, DMF and DMSO (Zhang *et al.*, 2015c). The results revealed that solvent molecules can enter the nanochannels formed by the tetrahedral–octahedral sheets of ATP, and this intercalation behaviour was found to depend primarily on solvent polarity (Barrer & Mackenzie, 1954). Strongly polar solvents such as DMSO and DMF were capable of intercalating into the channel structure of ATP, leading to shifts in the (110) diffraction peak and changes in its intensity, indicative of a pronounced intercalation effect. In contrast, solvents with lower polarity – namely MT, ET and IPA – tended to adsorb on the surface and exerted minimal influence on the crystal structure (Fig. 5d). In terms of morphological evolution, ATP treated with MT and DMF predominantly existed as individual rod-like crystals, whereas those treated with ET and IPA still retained some small-sized crystal bundles. Furthermore, carbon species were detected on the surface of the treated ATP, with the DMF-treated group exhibiting the highest carbon density, further confirming that solvent molecules underwent certain chemical or physical interactions with the crystal surface. The presence of CH_3-related vibrational bands in the infrared spectra also provided evidence for the residual attachment or grafting of solvent groups onto the ATP surface (Fig. 5e). Zeta-potential measurements (Fig. 5f) showed that pristine ATP had a potential of –25.5 mV, which increased to varying degrees after solvothermal treatment (e.g. –14.7 mV for IPA and –20.9 mV for DMF), reflecting changes in surface charge characteristics. These variations are closely associated with the modification of the electrical double layer and the adjustment of surface functional groups.

The solvothermal-modified, HCl-purified ATP in the presence of glycine (GLY) at 180°C, pH 12, at a solid-to-liquid ratio of 1:100, for 60 h can cleave the Si–O–Si and Si–O–*M* bonds, inducing crystal structure evolution (Zhang *et al.*, 2015b). Increasing GLY concentration progressively decreased the diffraction intensities of the ATP (110), (200) and (130) planes, indicating pronounced amorphization accompanied by silicate tetrahedral chain rearrangement and a reduced dolomite phase (Fig. 5g). Glycine concurrently reacted under hydrothermal conditions, grafting carboxyl (–COOH), amino ($-NH_2$) and carboxylate ($-COO^-$) groups onto the surface, increasing surface negative charge density and metal complexation capacity. Pristine ATP exhibited dense, rod-like crystal bundles; after modification, bundles disaggregated, rods shortened and a rod–sheet composite structure formed (Fig. 5h). Excessively high GLY concentrations induced excessive amorphization (Fig. 5i). These structural and morphological changes

https://doi.org/10.1180/clm.2026.10054 Published online by Cambridge University Press

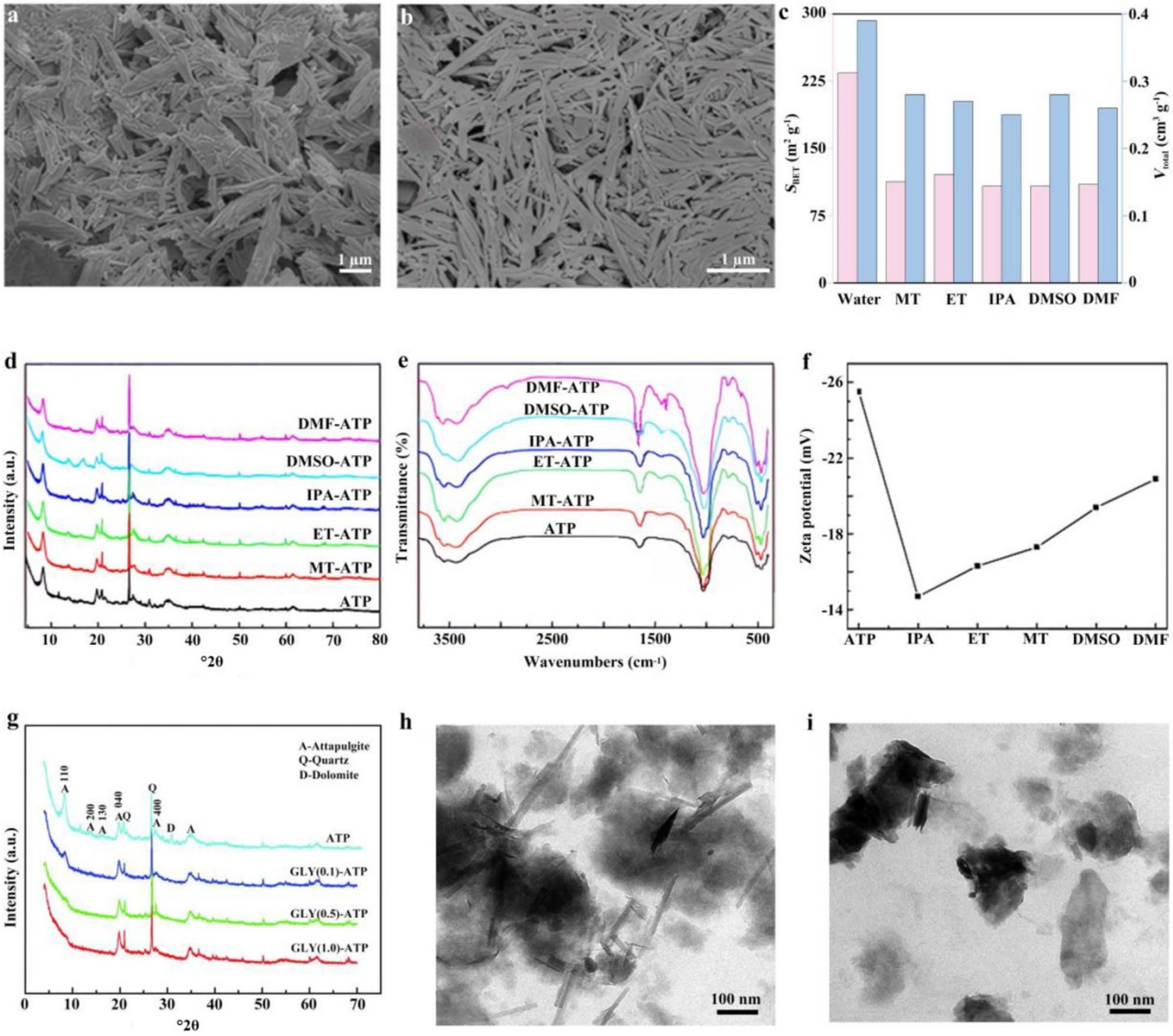


Figure 5. (a) Field-emission SEM (FESEM) image of natural ATP. (b) FESEM image of homogenized ATP dispersed in DMSO. (c) SSA and total pore volume of homogenized ATP in various liquid media (Xu *et al*., 2013b). (d) XRD traces, (e) Fourier-transform infrared spectroscopy and (f) zeta potential of pristine ATP and solvothermally treated ATP in various solvents (MT, ET, IPA, DMSO and DMF; Zhang *et al*., 2015c). (g) XRD traces of ATP, GLY(0.1)-ATP, GLY(0.5)-ATP and GLY(1.0)-ATP. (h) Transmission electron microscopy (TEM) image of GLY(0.5)-ATP. (i) TEM image of GLY(1.0)-ATP (Zhang *et al*., 2015b).

increase the density of accessible active sites and pore utilization efficiency.

Solvothermal treatment is an effective approach for regulating the dispersion behaviour, surface chemistry, pore structure and microstructural evolution of ATP through a solvent-involved reaction environment. Through solvent-assisted deagglomeration, channel intercalation, surface interaction and structural reconstruction, ATP can be modified to exhibit improved dispersibility, altered surface charge characteristics and increased accessibility of active sites. These changes provide an important basis for the controllable preparation of ATP with tailored physicochemical properties.

However, solvothermal treatment also has inherent limitations. The modification outcome is highly sensitive to solvent type and processing parameters, and the respective effects of solvent polarity, viscosity, vapour pressure and hydrogen-bonding capability have not yet been fully elucidated. Under inappropriate conditions, solvothermal treatment may result in insufficient deagglomeration, unstable surface modification, retention of solvent-derived species or excessive structural disorder and amorphization, thereby impairing the structural integrity of ATP. Future work should emphasize both mechanistic understanding and process controllability. In particular, systematic comparison of various solvent systems, together with analysis of their physicochemical properties, is needed to establish quantitative relationships between solvent characteristics and the resulting changes in ATP structure and properties. More attention should also be paid to distinguishing the respective roles of surface adsorption, channel intercalation, chemical association and framework reconstruction during solvothermal treatment. Furthermore, the recycling of residual solvent-derived species and their influence on the stability and reactivity of modified ATP require further clarification. From a practical perspective, the development of recyclable, low-toxicity and scalable solvent systems will be essential for expanding the

https://doi.org/10.1180/clm.2026.10054 Published online by Cambridge University Press

Table 2. Comparative advantages of ATP over representative fillers in functional coating applications.

Filler	Cost-effectiveness	Multifunctionality	Processability/dispersion	Stability
ATP	Low cost, abundant	Easy modification, enabling multiple functionalities	Compatible with conventional processing	Thermal and chemical stability
LDH	Moderate	Good ion-exchange capability but complex functionalization	Aggregation tendency, limited polymer compatibility	Acid-sensitive, prone to structural degradation under humid conditions
CNTs	High cost	Excellent mechanical properties but limited multifunctionality	Severe agglomeration	Structurally stable but dispersion-dependent
Graphene	High cost	Excellent barrier but limited functional integration	Restacking issues	Prone to oxidation and restacking
MOFs	Relatively high cost	Tuneable porosity and functionality	Compatibility issues with polymers	Stability concerns under humid or thermal conditions

applicability of solvothermal modification. Progress in these areas will support the more rational and controllable design of ATP with tailored structures and surface properties while also promoting the development of efficient and scalable modification processes.

Application of ATP-based coating

High-performance coatings rely significantly on high-quality functional fillers to improve their properties and performance. Despite the widespread use of various nanomaterials, current functional coatings still face challenges in active-agent immobilization, sustained performance, interfacial stability and multifunctional integration. Owing to its inherent channels, modifiable surface and good dispersibility, ATP can host active species (e.g. corrosion inhibitors, anti-bacterial agents and hydrophobic molecules) for controlled release and prolonged protection while also imparting functionalities such as self-cleaning, superhydrophobicity, anti-bacterial activity and anti-icing through surface and structural regulation. As shown in Table 2, compared to layered double hydroxides (LDHs), carbon nanotubes (CNTs), graphene and metal–organic frameworks (MOFs), ATP combines low cost, abundant availability, processing compatibility and structural stability, demonstrating strong potential for large-scale applications. Accordingly, this section focuses on modified ATP as a functional filler and micro/nano-container for developing functional coatings with self-healing, superhydrophobic, self-cleaning, anti-bacterial and anti-icing properties.

Superhydrophobic coatings

Superhydrophobic surfaces have garnered extensive attention over the past two decades due to their unique water-repellent characteristics, which impart self-cleaning and anti-fouling properties. Defined by a water contact angle (CA) exceeding 150° and a sliding angle (SA) below 10° (Wei *et al.*, 2023), these surfaces arise from the synergistic effect of specific micro/nano-scale topographic features and a low-surface-energy chemical composition. One-dimensional rod-shaped ATP possesses unique structural characteristics and abundant active sites for chemical modification, facilitating surface functionalization with silane coupling agents, polymers or inorganic nanoparticles. More importantly, ATP can self-assemble or undergo specific aggregation to form hierarchical micro/nanostructures, providing an ideal physical skeleton for constructing superhydrophobic surfaces that exhibit the Cassie–Baxter state.

Silane coupling agents are widely used to modify ATP so as to impart superhydrophobicity. The modification process involves hydrolysis of the silane coupling agent to generate hydroxyl groups, which subsequently react with the hydroxyl groups on the ATP surface, resulting in covalently bonded, silane-modified ATP. Commonly used silane coupling agents include long-chain alkylsilanes or fluorosilanes, which contain alkyl or fluorine functional groups that confer water-repellent properties (Zhang *et al.*, 2018a, 2024a; Dong *et al.*, 2023; Meng *et al.*, 2024; Wang *et al.*, 2025b). Numerous studies have employed fluorine-free silane coupling agents to modify ATP for superhydrophobic applications (Long *et al.*, 2020; Liu *et al.*, 2024; Wang *et al.*, 2024, 2025a; Zhang *et al.*, 2025b).

An ATP-based filler (BTA@SH-P-H, where BTA = benzotriazole and SH-P-H = natural ATP; Fig. 6a) was developed by modifying ATP with *n*-dodecyltrimethoxysilane (DTMS) and subsequently loading it with BTA (Wang *et al.*, 2025b). The hydrophobicity of the resulting coating was systematically investigated by adjusting the mass ratio of epoxy (EP) to fillers (Fig. 6b). When the ratio was below 0.8, the water CA remained at nearly 165° and the SA was close to 0°, with only slight variations observed for EP/BTA@SH-P and EP/BTA@SH-P-H. Further increasing the EP content caused the coating to lose its superhydrophobic properties, as the excess hydrophilic EP dominated the wettability of the composite coating. The hydrophobicity of the EP/BTA@SH-P-H coating after mechanical damage is shown in Fig. 6c. As the abrasion distance increased, the CA decreased and the SA increased due to deterioration of the rough structure and loss of coating components. When the abrasion distance reached 800 cm, the coating transitioned from a superhydrophobic to a hydrophobic state. Additionally, after 10 min of high-velocity water impact (25 kPa), the CA and SA of the coating were 155.0° ± 0.89° and 4.0° ± 0.43°, respectively (Fig. 6d). Following chemical durability testing (92 h of immersion; Fig. 6e) and ultraviolet (UV) resistance testing (Fig. 6f), the coating maintained its superhydrophobic state, indicating good chemical stability and suitability for long-term practical applications.

Fluorine-containing silane coupling agents have also been used as modifiers for ATP. A double-layer coating was designed to protect AZ31B Mg alloy, consisting of a bottom layer of BTA-doped shape memory polymer (SMP) and a top layer of 1H,1H,2H,2H-perfluorodecyltriethoxysilane-modified ATP (Zhang *et al.*, 2021). The solid–liquid contact time during the first impact/bounce process was 12.5 ms for a 3.5 wt.% NaCl droplet and 16.5 ms for an *n*-hexadecane droplet (Fig. 6g,h). After long-term immersion

https://doi.org/10.1180/clm.2026.10054 Published online by Cambridge University Press

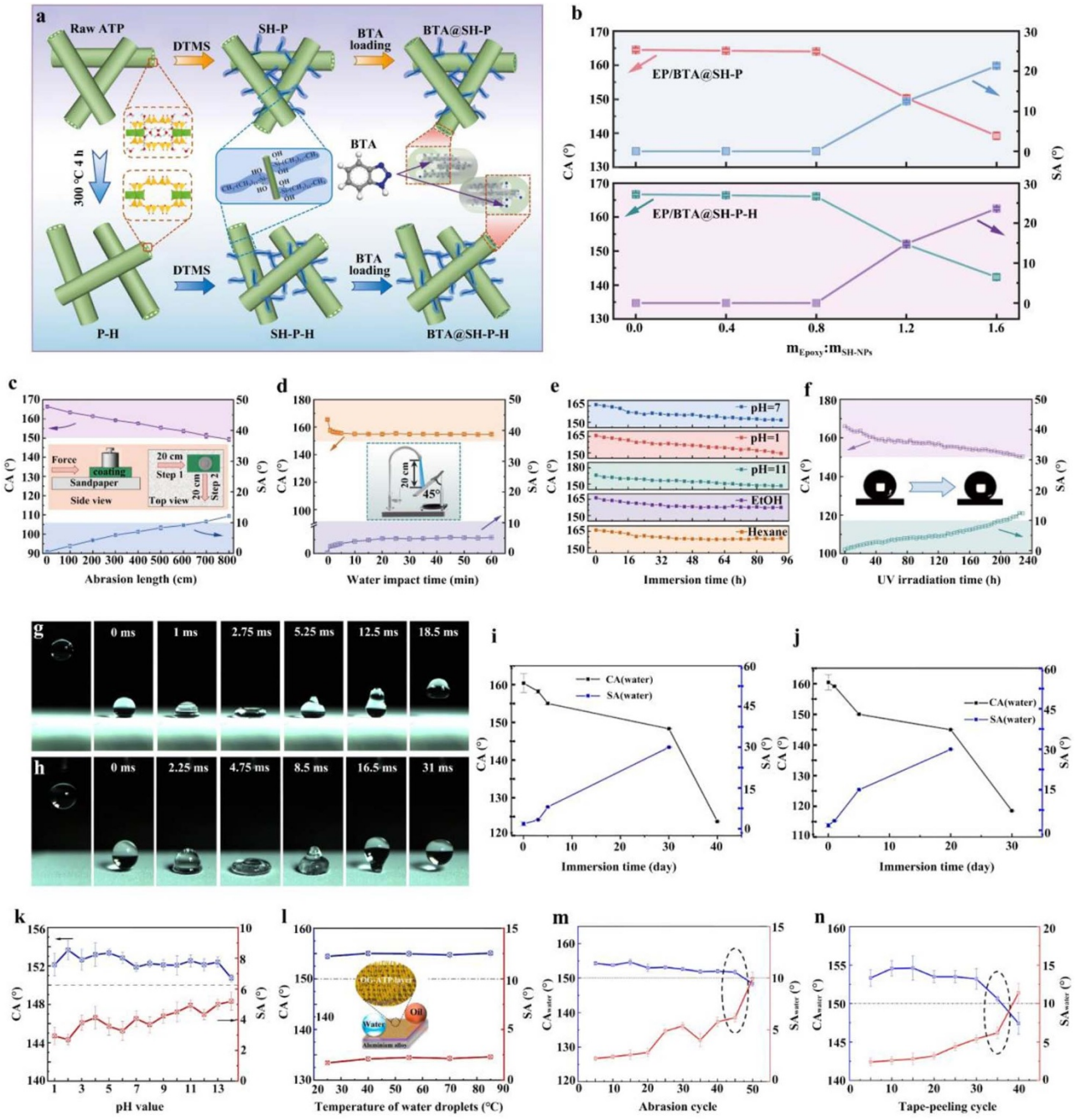


Figure 6. (a) Schematic illustration of the preparation process for BTA-loaded superhydrophobic ATP containers. (b) Water CA and SA of composite coatings as a function of the EP resin to superhydrophobic nanoparticle mass ratio (thermally untreated SH-P and 300°C-activated SH-P-H; Wang *et al*., 2025b). (c,d) Evolution of CA and SA during (c) sandpaper abrasion and (d) water impact testing (Wang *et al*., 2025b). (e) CA of the EP/BTA@SH-P-H coating as a function of immersion time in various media: organic solvents (ethanol and *n*-hexane), acidic solution (pH 1), alkaline solution (pH 14) and saline solution (3.5 wt.% NaCl, pH 7; Wang *et al*., 2025b). (f) CA and SA of the coating as a function of UV irradiation time (Wang *et al*., 2025b). (g,h) Photographs of the SMP-BTA/fluoro-ATP-coated Mg alloy showing the impact and rebound behaviour of (g) a 3.5 wt.% NaCl droplet and (h) an *n*-hexadecane droplet (10 μL; Zhang *et al*., 2021). (i,j) Variation in superhydrophobicity of the SMP-BTA/ATP coating during (i) immersion testing and (j) neutral salt spray testing (Zhang *et al*., 2021). (k,l) CA and SA of the superamphiphobic OG-ATP/EP bilayer coating measured with droplets of (k) different pH values and (l) different temperatures (Zhang *et al*., 2024a). (m,n) CA and SA of water and *n*-hexadecane on the superamphiphobic bilayer coating after (m) sandpaper abrasion and (n) tape-peeling cycles (Zhang *et al*., 2024a).

(30 days; Fig. 6i) and salt spray testing (5 days; Fig. 6j), the SMP-BTA/fluoro-ATP coating remained superhydrophobic, with a SA below 15°. With extended measurement time, the coating transitioned to a hydrophobic state with a SA exceeding 30°. Similarly, a bilayer coating was prepared on 5083 aluminium alloy (Zhang *et al*., 2024a) comprising a bottom EP layer and a top organosilane-grafted ATP layer (OG-ATP/EP). The superamphiphobicity of the OG-ATP/EP coating was evaluated using acidic, alkaline and high-temperature water droplets. The results (Fig. 6k) showed that droplets with pH values ranging from 1 to 14 exhibited a CA greater than 150° and a SA below 5.5°. For high-temperature water droplets (25–85°C), the CA ranged from 154°

https://doi.org/10.1180/clm.2026.10054 Published online by Cambridge University Press

to 156° and the SA remained below 2.5° (Fig. 6l). The hydrophobicity of the OG-ATP/EP coating was further evaluated in terms of mechanical stability and surface adhesion. The results indicated that even after 45 cycles of sandpaper abrasion (Fig. 6m) and 35 cycles of tape-peeling tests (Fig. 6n), the coating retained its superhydrophobic properties.

In summary, leveraging its one-dimensional nano-structural characteristics, the core functions of ATP in superhydrophobic coatings are manifested as follows: (1) the nanorod framework constructs a hierarchical micro/nano-rough surface for air layer entrapment; (2) surface hydroxyl groups facilitate chemical modification to introduce low-surface-energy moieties and increase interfacial compatibility; and (3) synergistic interaction with the coating matrix improves mechanical stability and structural robustness. This 'morphology–chemistry' synergy mechanism provides a general strategy for achieving the Cassie–Baxter state and optimizing overall performance.

Despite significant progress in the design of ATP-based superhydrophobic coatings, several challenges persist. First, the long-term stability of coatings in complex environments remains insufficient, as micro/nano-structures are susceptible to damage. Second, the potential environmental risks associated with fluorine-containing modifiers urgently need to be addressed. Third, the adaptation of scalable fabrication processes to practical application scenarios requires further optimization. Fourth, the degree of multifunctional integration needs to be improved.

Future research directions should focus on the following areas: (1) developing green modifiers, such as natural plant extracts and bio-based polymers, to achieve fluorine-free and environmentally friendly modification; (2) optimizing coating structural design and incorporating self-healing components to improve mechanical stability and long-term service life; (3) expanding towards multifunctional integrated coatings with photothermal, conductive or antibacterial properties to meet complex application demands; and (4) simultaneously developing green, efficient, one-step modification processes and scalable coating technologies to move ATP-based superhydrophobic materials towards practical applications.

Active corrosion protection coating

The application of ATP in anticorrosion coatings primarily manifests in two aspects: enhancing the physical barrier effect and enabling active corrosion protection through the storage and controlled release of corrosion inhibitors (Liu *et al.*, 2018a,b; Li *et al.*, 2025). The evolution of this application involves transitioning pristine and modified ATP from a passive physical barrier to an ATP-based micro/nano-container designed for active corrosion protection (Lu & Wang, 2022; Wu *et al.*, 2023b). Owing to the high aspect ratio of its nanorod structure, ATP creates a more tortuous diffusion pathway for corrosive species (e.g. H_2O, O_2 and Cl^-) within the coating matrix, thereby effectively retarding their penetration towards the metal–coating interface (Nan *et al.*, 2019; Li & Nan, 2023). Concurrently, the intrinsic tubular channels of ATP serve as ideal micro/nano-containers for encapsulating corrosion inhibitors, which can be released upon local coating damage to mitigate corrosion of the metallic substrate (AïtAghzzaf *et al.*, 2017; Ni *et al.*, 2021; Xue *et al.*, 2022; Yu *et al.*, 2022; Butt *et al.*, 2023; Ali *et al.*, 2024, 2025a,b; Gao *et al.*, 2025; Wang *et al.*, 2025b; Xu *et al.*, 2025).

Research on ATP-based micro/nano-containers focuses on optimizing the porosity structure of ATP, regulating inhibitor release behaviour and elucidating the mechanisms of active corrosion protection (Thomas *et al.*, 2022; Udoh *et al.*, 2024). For example, a ULM@ATP/Oil-2 (5.0 wt.% ULM@ATP in silicone oil; ULM = 2-undecylimidazoline) anti-corrosive coating was developed, and incorporating ULM@ATP composites was demonstrated to markedly improve the corrosion resistance of the coating (Fig. 7a; Wu *et al.*, 2023b). Specifically, after 480 h of immersion in a 3.5 wt.% NaCl solution, the low-frequency impedance modulus ($|Z|_{0.01Hz}$) of the ULM@ATP/Oil-2 coating remained as high as 1.62×10^8 Ω·cm^2 (Fig. 7b), approximately three orders of magnitude higher than that of the pure oil coating. Moreover, the introduction of ULM significantly improved the dispersion of ATP within the coating matrix. ATP particles, which originally exhibited a strong tendency to form sheet-like aggregates, were effectively dissociated after ULM loading, resulting in a more uniform and well-dispersed microstructure (Fig. 7c).

Building on this concept, ATP was successfully loaded with 3-amino-1,2,4-triazole-5-thiol (ATAT) to construct inhibitor-containing nanofillers (ATP@ATAT), which were then incorporated into an epoxy matrix to provide both active and passive corrosion protection for metallic substrates (Ali *et al.*, 2026). Electrochemical impedance spectroscopy demonstrated that the $|Z|_{0.01Hz}$ of the composite coating containing 3 wt.% ATP@ATAT reached as high as 7.6×10^9 Ω·cm^2 after 120 days of immersion, nearly two orders of magnitude higher than that of the neat epoxy coating (5.69×10^7 Ω·cm^2), indicating a substantially improved barrier effect (Fig. 7d). The adhesion strength of the epoxy coating containing 3 wt.% ATP@ATAT was significantly improved from 3.10 to 4.95 MPa (Fig. 7e). Furthermore, the ATP@ATAT system exhibited pH-responsive release behaviour (Fig. 7f), enabling rapid and controlled release of ATAT under alkaline conditions associated with localized corrosion, thereby highlighting its strong potential for self-healing protective coatings. SEM images revealed that, after scratch immersion, the EP/ATP@ATAT-3% coating exhibited the least loss of surface integrity, demonstrating that the active protection endowed by the ATP@ATAT composite effectively suppressed the corrosion process and restrained the growth of corrosion products (Fig. 7g). This corrosion protection mechanism can be attributed to the synergistic effect of ATP nanofillers and the released ATAT passivating the damaged region.

A pH-responsive ATP nanocontainer was developed in which BTA was loaded *via* a layer-by-layer self-assembly strategy (Liu *et al.*, 2018b). For the scratched epoxy coating incorporating the assembled ATP nanoparticles, the scanning electrochemical microscopy (SECM) probe current at the defect increased from 0.3 to 1.2 nA with increasing immersion time (Fig. 7j,k), markedly higher than that recorded for the scratched epoxy coating without assembled ATP nanoparticles (Fig. 7h,i). This increased current indicates a reduction in corrosion activity within the scratched area, attributed to the release of BTA from the assembled ATP, which formed an adsorbed protective layer on the metal surface and thereby suppressed corrosion kinetics.

In another study, an ATP@IL/EP (IL = 1-allyl-3-octylimidazolium bromide; EP = epoxy) coating was prepared and tested for its salt spray performance (Ci *et al.*, 2022). Following the ASTM B117 standard, coating samples with an artificial scratch of ~10 cm in width were exposed to a neutral salt spray environment. After 7 and 14 days of exposure, the ATP@IL/EP coating (Fig. 7l–n) exhibited significantly better corrosion resistance than the reference samples, demonstrating excellent anticorrosion performance. Regardless of the type of ATP-based micro/nano-container, the underlying corrosion protection mechanism (Yu *et al.*, 2022) involves the release of corrosion inhibitors to passivate defect sites (Fig. 7o).

https://doi.org/10.1180/clm.2026.10054 Published online by Cambridge University Press

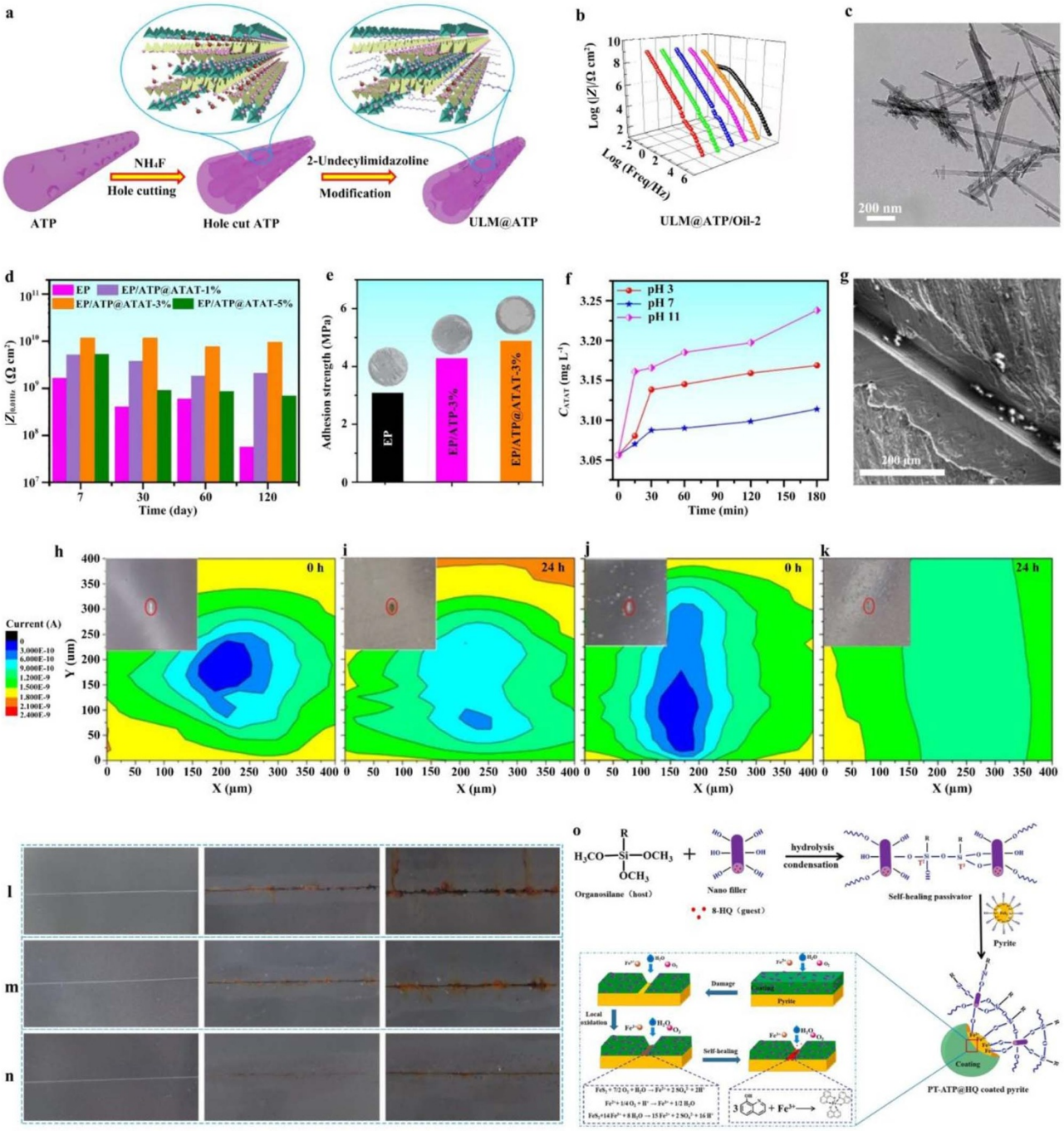


Figure 7. (a) Schematic illustration of the synthesis of ULM@ATP. (b) $|Z|_{0.01Hz}$ of the ULM@ATP/Oil-2 coating after 480 h of immersion in 3.5 wt.% NaCl solution. (c) Transmission electron microscopy image of ULM@ATP (Wu *et al.*, 2023b). (d) $|Z|_{0.01Hz}$ values of various composite coatings. (e) Pull-off adhesion strengths of various composite coatings. (f) pH-responsive release profile of ATP@ATAT. (g) SEM image of the peeled EP/ATP@ATAT-3% coating after 96 h of immersion in 3.5 wt.% NaCl solution (Ali *et al.*, 2026). (h–k) SECM maps of (h,i) a defective blank coating and (j,k) an assembled ATP coating on carbon steel immersed in electrolyte solution (Liu *et al.*, 2018b). (l–n) Photographs of coatings after salt spray testing: (l) pure EP, (m) ATP/EP and (n) ATP@IL/EP (Ci *et al.*, 2022). (o) Schematic illustration of the passivation and self-healing mechanism of PT-ATP@HQ for pyrite (Yu *et al.*, 2022). HQ: 8-hydroxyquinoline (corrosion inhibitor); PT = organosilane passivator (Prop-SH/TEOS).

This discussion clearly demonstrates that ATP-based anticorrosion coatings significantly improve both corrosion protection performance and damage-induced self-healing ability through the synergistic coupling of physical barrier action and triggered inhibitor release-induced interfacial passivation. Nevertheless, the development of ATP-based micro/nano-container anticorrosion coatings still faces three major challenges. First, precise regulation of micro/nano-container loading capacity and release kinetics remains to be achieved. Second, the long-term service stability of such coatings under multi-field coupled environments (e.g. salt spray, ultraviolet irradiation and freeze–thaw cycling) requires systematic evaluation. Third, the engineering compatibility of green

https://doi.org/10.1180/clm.2026.10054 Published online by Cambridge University Press

corrosion inhibitor systems with waterborne or solvent-free processes needs further improvement.

Future research should pursue deeper interdisciplinary integration. On the one hand, *in situ* electrochemical characterization combined with molecular dynamics simulation should be employed to elucidate the dynamic interaction mechanisms at the ATP–inhibitor–metal interface. On the other hand, multi-stimuli-responsive release systems triggered by Cl^-, pH and temperature should be developed to improve environmental specificity and response precision for intelligent protection. In parallel, the green integration of bio-based corrosion inhibitors with environmentally friendly resin systems should be actively promoted to accelerate the development of ATP-based anticorrosion coatings towards higher performance, greater intelligence and improved sustainability.

Anti-bacterial/anti-fouling coating

ATP, endowed with a distinctive one-dimensional nanorod architecture, tuneable surface chemistry and high SSA, exhibits exceptional proficiency in immobilizing nanoparticles and small organic molecules (Galán *et al*., 1994; Lei *et al*., 2017; Zhong *et al*., 2020; Gao *et al*., 2024; Liu *et al*., 2025), establishing itself as a highly promising platform for engineering high-performance, intelligent anti-bacterial/anti-fouling coatings. ATP not only facilitates superhydrophobicity for bacterial anti-adhesion through micro/nano-hierarchical structuring combined with low-surface-energy modification (Hizal *et al*., 2017; Li *et al*., 2018; Liu *et al*., 2021; Zhan *et al*., 2022; Wu *et al*., 2023b) but also functions as an efficient micro/nano-container for the controlled release of anti-bacterial agents. Critically, its sharp nanorod morphology confers a chemical reagent-independent physical bactericidal capability. The synergistic interplay of these three mechanisms – physical barrier, sustained release and mechanical disruption – significantly enhances both protective efficacy and environmental sustainability.

Current research on ATP-based anti-bacterial composites predominantly explores two pathways: (1) ATP composites with metal ions (Ag^+, Cu^{2+} and Zn^{2+}) and metal oxides demonstrate long-lasting anti-bacterial activity and stability for releasing metal ions, achieving the dual functionality of bacterial inhibition and adsorption (Zhao *et al*., 2006; Huo & Yang, 2010; Yang *et al*., 2011); and (2) ATP loaded with anti-bacterial agents (e.g. quaternary ammonium compounds, quaternary phosphonium salts, benzophenone derivatives, imidazolidinyl urea, pyrithione-based compounds and natural phenolic compounds) enables the controlled release of anti-bacterial agents and achieves increased biocidal efficiency (Cai *et al*., 2013).

Numerous studies (Zhao *et al*., 2006; Huo & Yang, 2010; Yang *et al*., 2011; Cai *et al*., 2013; Zhong *et al*., 2020; Jiang *et al*., 2024; Liu *et al*., 2025) have reported the utilization of ATP as a support matrix for the incorporation of organic or inorganic biocides in the formulation of anti-bacterial and anti-fouling coatings. For organic anti-bacterial agents, Zhong *et al.* (2020) developed a green and facile strategy to load carvacrol (CAR) – a natural essential oil – onto ATP to obtain CAR/ATP *via* mechanical milling. The CAR/ATP exhibited a high loading capacity (23.00%) and sustained release behaviour, effectively overcoming the volatility and low solubility of CAR. The CAR/ATP anti-bacterial materials demonstrated effective anti-bacterial activity against both *Escherichia coli* and *Staphylococcus aureus*, with a minimum inhibitory concentration (MIC) of 2.0 mg mL^{-1}. This work highlights the potential of ATP as a micro/nano-container for natural, low-toxicity anti-bacterial agents, which is particularly advantageous for environmentally benign anti-fouling coatings requiring long-term controlled release.

Liu *et al.* (2025) used ATP as a micro/nano-container to immobilize anti-bacterial components (dodecyl glycoside quaternary ammonium salt; APGQAS) through its strong adsorption capacity. Subsequently, copper tannate (CuTA) was *in situ* synthesized on the modified ATP and incorporated into Paraloid B72 to form the CuTA/APT@APGQAS/B72 composite coating. Anti-bacterial tests showed that at a concentration of 2 mg mL^{-1}, this coating achieved inhibition rates of 99.99% against *E. coli* and 98.76% against *S. aureus*. The composite coating with 4 wt.% nanofiller reached 99.98% anti-bacterial efficiency against *E. coli*, and at 5 wt.% loading it reached over 99% inhibition against *S. aureus*. The synergistic anti-bacterial mechanisms involve the released Cu^{2+} disrupting bacterial membranes, tannic acid-derived polyphenols inducing oxidative stress and blocking metabolism and surface-grafted quaternary ammonium salts damaging cell walls.

Addressing the dual challenges of bacterial contamination and biofouling, the integration of 'passive anti-adhesion + active anti-bacterial' strategies has emerged as a cornerstone of green anti-fouling design. A previous study pioneered a bifunctional filler system using ATP as the structural scaffold: PSF (silica-decorated ATP) and FTAP (tannic acid-mediated Ag nanoparticle-anchored ATP) were co-dispersed in fluorosilicone resin to fabricate the FPFTS superhydrophobic anti-bacterial coating (Fig. 8a; Jiang *et al*., 2024). Quantitatively, bacterial adhesion of *E. coli* and *S. aureus* was reduced by 79.7 ± 6.2% and 81.9 ± 2.0%, respectively, compared to the blank sample (Fig. 8b,d), while inactivation rates reached 100.0 ± 0.1% and 99.8 ± 0.1%, respectively (Fig. 8c,e), attributable to the synergy of nanorod-induced membrane piercing and Ag^+/reactive oxygen species (ROS)-mediated chemical eradication. Notably, the Cassie-state air film dynamically modulated Ag^+ release kinetics (Fig. 8f), preventing burst release and minimizing ecological impact. Mechanistically, the coating unified passive defence (air film-mediated adhesion suppression and physical piercing) and active killing (Ag^+-induced osmotic disruption, thiol protein inactivation, DNA interference and ROS-driven lipid peroxidation), establishing a reproducible blueprint for eco-friendly, intelligent anti-fouling systems (Fig. 8g–i).

Collectively, the role of ATP in anti-bacterial coatings has evolved far beyond that of a passive filler. In early-stage systems, ATP mainly served as a container for the immobilization and controlled release of biocidal agents. Subsequent studies increasingly exploited its intrinsic one-dimensional nanorod morphology to construct micro/nano-rough surfaces for anti-adhesion and to induce direct mechanical damage to bacterial membranes, thereby transforming ATP from a 'supporting component' into a 'structure-enabled functional unit'. More recently, ATP has been further integrated into multifunctional nanozyme and catalytic sterilization systems, where its surface chemistry, interfacial charge characteristics and hierarchical architecture collectively regulate nanoparticle dispersion, ion-release behaviour and reactive species generation. This progression reflects a fundamental shift in ATP-based coating design: from simply incorporating anti-bacterial additives into a matrix towards deliberately engineering ATP as a multifunctional platform that couples surface topography, interfacial chemistry and bioactive response.

Future research should therefore move beyond empirical material combination and focus on three key directions: (1) precise control of ATP surface/interface chemistry; (2) quantitative understanding of the relationship between nanorod assembly and anti-bacterial performance; and (3) the development of

https://doi.org/10.1180/clm.2026.10054 Published online by Cambridge University Press

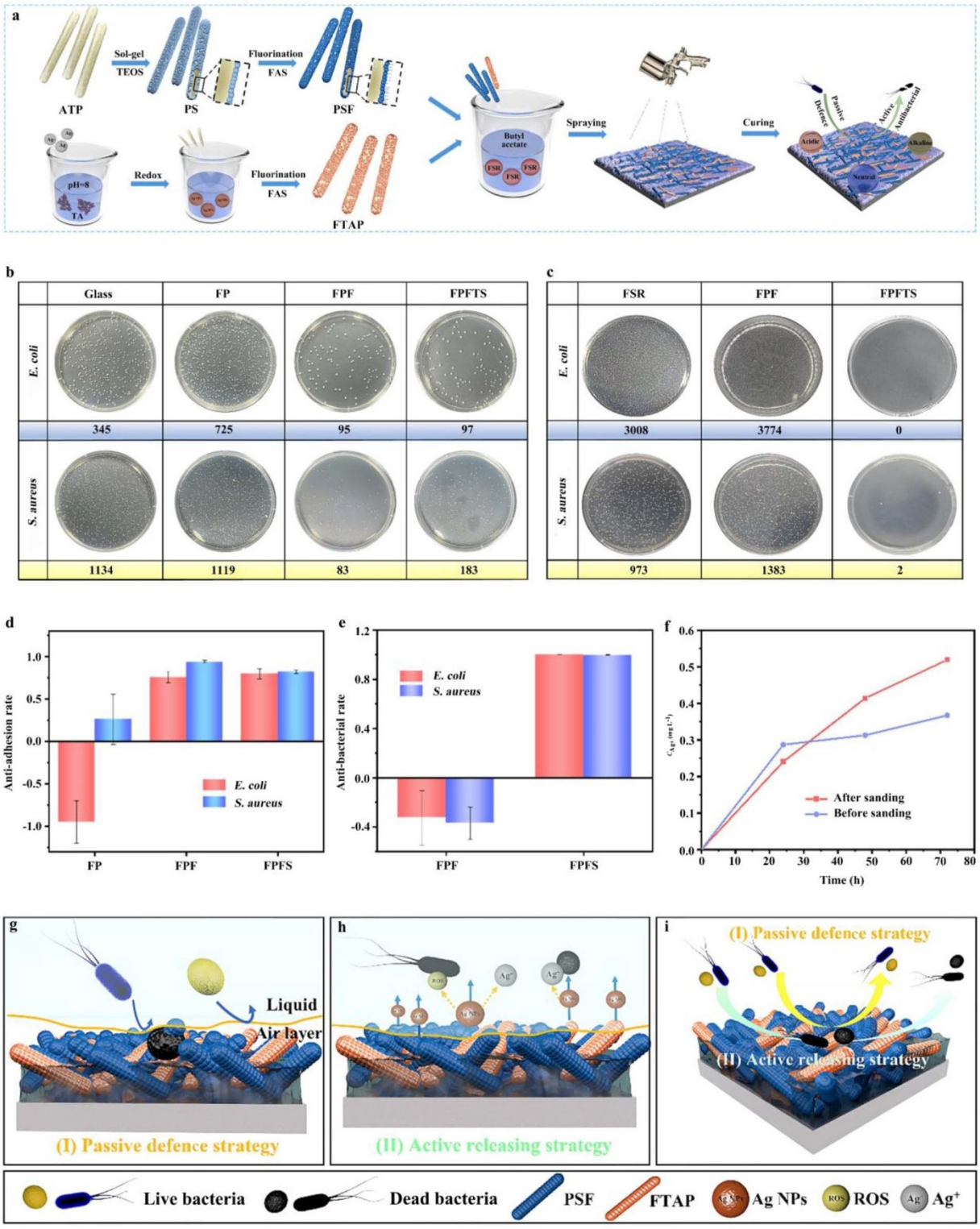


Figure 8. (a) Schematic illustration of the fabrication process for the FPFTS coating. (b) Bacterial adhesion colonies on agar plates for various surfaces and (c) bacterial colonies on agar plates for various surfaces in anti-bacterial experiments. The numbers below the images denote colony-forming units (blue: *E. coli*; yellow: *S. aureus*). (d) Anti-adhesion performance of various material surfaces. (e) Anti-bacterial rates of various material surfaces. (f) Ag^{+} concentration in the soaking solution before and after wear resistance testing. (g) Schematic illustration of the passive defence mechanism of the FPFTS coating against bacteria. (h) Schematic illustration of the active anti-bacterial mechanism of the FPFTS coating. (i) Schematic illustration of the synergistic anti-bacterial mechanism of the superhydrophobic coating combining passive defence and active anti-bacterial strategies (Jiang *et al*., 2024). NP = nanoparticle.

https://doi.org/10.1180/clm.2026.10054 Published online by Cambridge University Press

stimuli-responsive ATP-based coatings capable of adaptive anti-fouling and on-demand sterilization under complex conditions. With these advances, ATP – as a naturally abundant and sustainable mineral nanomaterial – is expected to play an increasingly important role in next-generation, environmentally benign antibacterial and anti-fouling coatings.

Self-cleaning/anti-smudge coating

Self-cleaning/anti-smudge coatings are surface treatments capable of removing contaminants such as liquids, dirt, oil and other pollutants, thereby reducing surface smudging and facilitating easier cleaning. They generally achieve this by endowing the coating surface with superhydrophobicity, oleophobicity or superamphiphobicity – characteristics commonly obtained by constructing micro/nano-hierarchical structures and modifying rough surfaces with low-surface-energy substances (Ma & Hill, 2006; Rao *et al.*, 2009; Si & Guo, 2015; Yu *et al.*, 2018; Wang *et al.*, 2019b, 2020a, 2024, 2025b; Hooda *et al.*, 2020; Barthwal *et al.*, 2022; Guo *et al.*, 2022; Wei *et al.*, 2022; Butt *et al.*, 2023; Li *et al.*, 2023; Zhang *et al.*, 2024a).

An environmentally friendly and abrasion-resistant superhydrophobic anti-corrosion coating was prepared by doping hexadecyltrimethoxysilane (HDTMS)-modified ATP fillers in waterborne epoxy resin (Fig. 9a; Liu *et al.*, 2024). Copper chloride dihydrate, sand grains and silica powder were used as contaminants and uniformly dispersed on the surface of an inclined ATP@HDTMS@WEP (HDTMS-modified ATP as a filler combined with waterborne epoxy (WEP)) coating. Water droplets were then dropped onto the contaminated surface to observe their contaminant removal ability. The results indicated that all contaminants were removed without leaving water droplet traces (Fig. 9b). The self-cleaning mechanism of the ATP@HDTMS@WEP coating relies on its extremely low surface energy, which enables water droplets to roll off the surface, thereby removing surface contaminants. In addition, anti-smudge performance was further investigated using water, milk, tea and Coca-Cola. The ATP@HDTMS@WEP coatings were vertically dipped into the corresponding solutions for several seconds and then removed to observe surface contamination. After three repeated cycles, the surface remained clean and liquid non-wetting (Fig. 9c). These excellent anti-smudge and self-cleaning functions can be attributed to the air cushion present on the coating surface, which effectively decreases the contact area between liquids/solids and the coating.

To further improve self-cleaning/anti-smudge performance, a superamphiphobic coating was investigated (Zhang *et al.*, 2024b). A filler co-modified with TEOS and 1H,1H,2H,2H-perfluorooctyltriethoxysilane (PFAS) was prepared (OG-ATP; Fig. 9d), yielding a superamphiphobic material (Fig. 9e). The superamphiphobic self-cleaning effect of the OG-ATP coating was investigated using water and *n*-hexadecane droplets. Copper sulfate pentahydrate contaminant was evenly sprinkled on the coating surface. The results showed that both water and *n*-hexadecane droplets could remove the contaminant from the sample surface (Fig. 9f). Furthermore, water and various oil droplets on the OG-ATP coating surface exhibited superamphiphobic characteristics (Fig. 9g). The anti-smudge performance of the OG-ATP coating was evaluated using water, glycerol, ethylene glycol, peanut oil and *n*-hexadecane (Fig. 9h). No liquid residue was observed on the OG-ATP coating surface for any of the test liquids, demonstrating excellent liquid repellency and low interfacial adhesion. This non-wettability and liquid repellency are attributed to the rough structure of the OG-ATP coating and the ultra-low surface energy imparted by organosilane modification.

Although ATP-based self-cleaning/anti-smudge coatings exhibit excellent contaminant removal through the incorporation of modified ATP fillers, several challenges remain to be addressed. First is their insufficient mechanical durability. The superamphiphobic characteristics of the coatings are imparted by micro/nano-structures on their surface, which are easily damaged and cannot ensure long-term effectiveness. Second are their environmental concerns and high cost. Fluorinated fillers pose adverse environmental effects and incur high costs, while fluorine-free alternatives still cannot meet practical application requirements due to their inferior performance or durability. Future research should focus on developing multifunctional coatings with eco-friendly and sustainable fillers, as well as cost-effective manufacturing methods, to meet the demands of self-cleaning/anti-smudge coatings under harsh conditions.

Anti-icing coating

Superhydrophobic coatings represent one of the most promising passive anti-icing strategies (Long *et al.*, 2020; Zhang *et al.*, 2024a,b, 2025b; Wang *et al.*, 2025c). Their characteristics – high CA and low SA – reduce the solid–liquid contact area, thereby effectively delaying the icing process and diminishing ice adhesion strength (Kreder *et al.*, 2016; Wang *et al.*, 2022). The nanorod crystal structure of ATP provides a natural skeleton for constructing the micro/nano-scale rough topography required for superhydrophobic coatings. However, superhydrophobic anti-icing coatings can only delay icing; they cannot fundamentally prevent its occurrence. Once ice accumulates on the coating surface, the difficulty of de-icing becomes comparable to that of conventional coatings. Consequently, photothermal superhydrophobic coatings that integrate both passive anti-icing and active de-icing functionalities have emerged as an efficient and sustainable solution for ice prevention and removal (Jiang *et al.*, 2018; Cong *et al.*, 2023; Xie *et al.*, 2023b).

Through suitable modification of ATP fillers, coatings can be endowed with excellent passive anti-icing and active de-icing functions. Several studies have indicated that modifying ATP with silane coupling agents or carbon materials imparts excellent superhydrophobic and photothermal properties (Xie *et al.*, 2022; Mao *et al.*, 2024b). A PPy/ATP@hexadecylPOS (PPy = polypyrrole; hexadecylPOS = hexadecyl polysiloxane) filler (Xie *et al.*, 2022) was prepared through the oxidative polymerization of pyrrole on ATP, followed by modification with hexadecyl polysiloxane (Fig. 10a). Anti/de-icing coatings were then prepared by spray-coating a mixture of the PPy/ATP@hexadecylPOS filler and a silicone resin onto aluminium plates. The resulting coating exhibited superior superhydrophobicity, with a water CA of 162.7° and a SA of 2.7° (Fig. 10b). The coating demonstrated outstanding photothermal conversion efficiency: its surface temperature rapidly increased to 60.0°C after 1 min of irradiation, to 70.7°C after 3 min of irradiation and to 80.0°C after 10 min of irradiation – twice that of the pristine ATP coating (Fig. 10c). This rapid temperature rise facilitates the quick melting of transient ice layers, enabling active de-icing. Regarding passive anti-icing performance (in the dark, –10°C, 60% relative humidity), water droplets on bare aluminium completely froze in only 68 s, whereas those on the PPy/ATP@hexadecylPOS coating took nearly five times longer (330 s; Fig. 10d). For active anti-icing (1 sun, –10°C, 60% relative humidity), droplets on bare aluminium froze completely within 120 s, but freezing was delayed

https://doi.org/10.1180/clm.2026.10054 Published online by Cambridge University Press

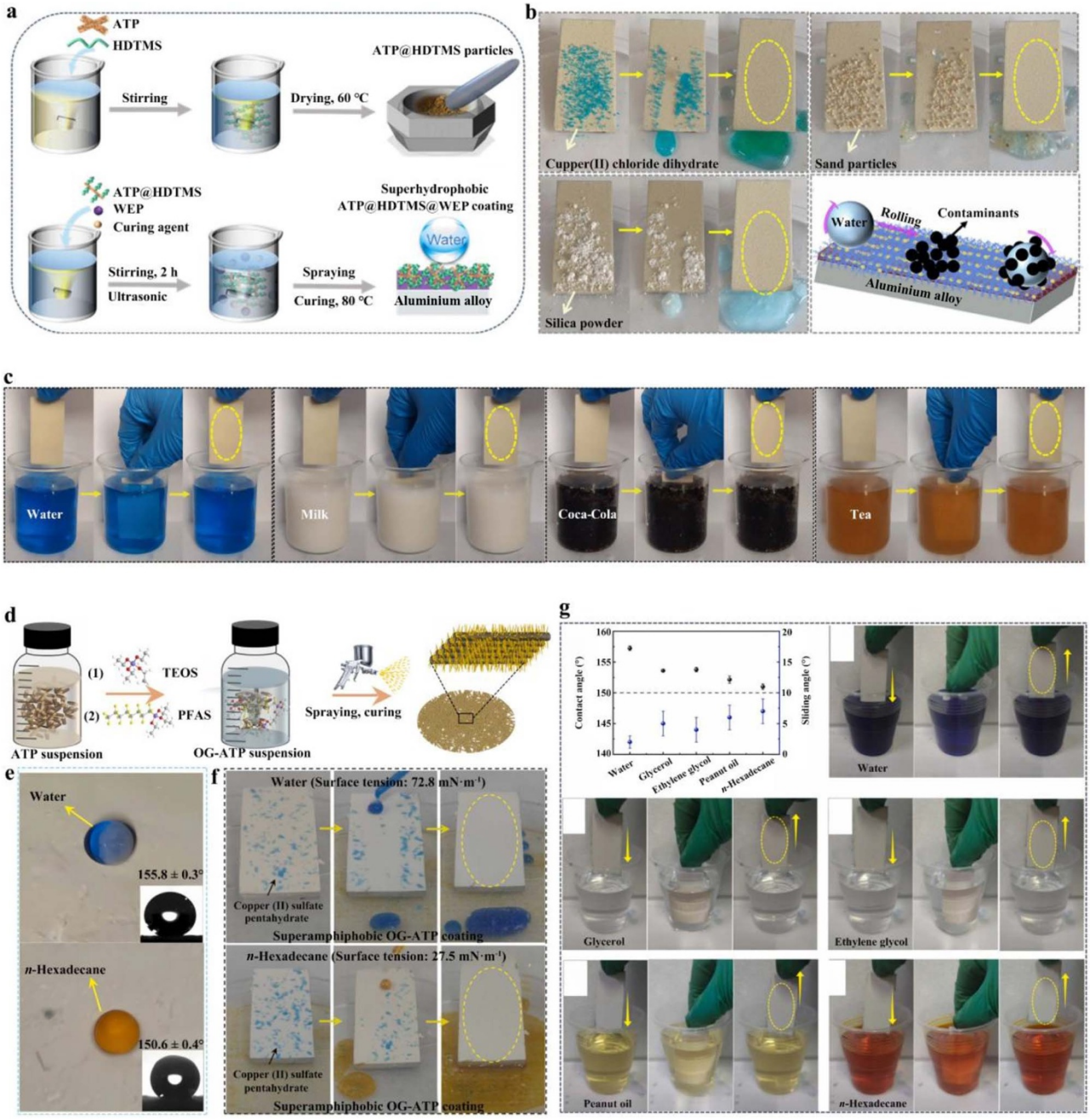


Figure 9. (a) Schematic illustration of the fabrication process for modified ATP@HDTMS particles and the superhydrophobic ATP@HDTMS@WEP coating. (b) Self-cleaning performance of the superhydrophobic ATP@HDTMS@WEP coating against various solid contaminants and the corresponding self-cleaning mechanism. (c) Anti-smudge performance of the superhydrophobic ATP@HDTMS@WEP coating against various liquid contaminants (Liu *et al.*, 2024). (d) Schematic illustration of the fabrication process for OG-ATP particles and the superamphiphobic coating. (e) Water droplet (surface tension at 20°C: 72.8 mN m^{-1}) and *n*-hexadecane droplet (surface tension at 20°C: 27.5 mN m^{-1}) on OG-ATP particles. (f) Self-cleaning evaluation of the superamphiphobic OG-ATP coating driven by water and *n*-hexadecane. (g) CA and SA values of various liquid droplets on the superamphiphobic OG-ATP coating, along with its anti-smudge performance against various liquid contaminants of different surface tensions (Zhang *et al.*, 2024b).

to 600 s on the coated aluminium (Fig. 10e), demonstrating exceptional photothermal conversion capability. The anti-icing mechanism of the coating arises from the synergistic effect between superhydrophobicity and the photothermal effect: (1) the three-level hierarchical micro/nano-structure and low surface energy significantly reduce the water–solid contact area and contact time *via* an insulating air cushion at the interface, thereby delaying the icing process and achieving efficient passive anti-icing; and (2) the PPy photothermal layer, supported by ATP, rapidly converts solar energy into thermal energy for active de-icing.

Similarly, a photothermal superhydrophobic coating (SiP/F-MOFs@ATP; SiP = silicone-modified polyester; F-MOFs = fluorinated MOFs) featuring a three-level micro/nano/nano-hierarchical structure based on ATP nanorods has been reported (Fig. 10f; Mao *et al.*, 2024b). The morphology of F-MOFs@ATP is shown in Fig. 10g. The coating exhibited a surface roughness

https://doi.org/10.1180/clm.2026.10054 Published online by Cambridge University Press

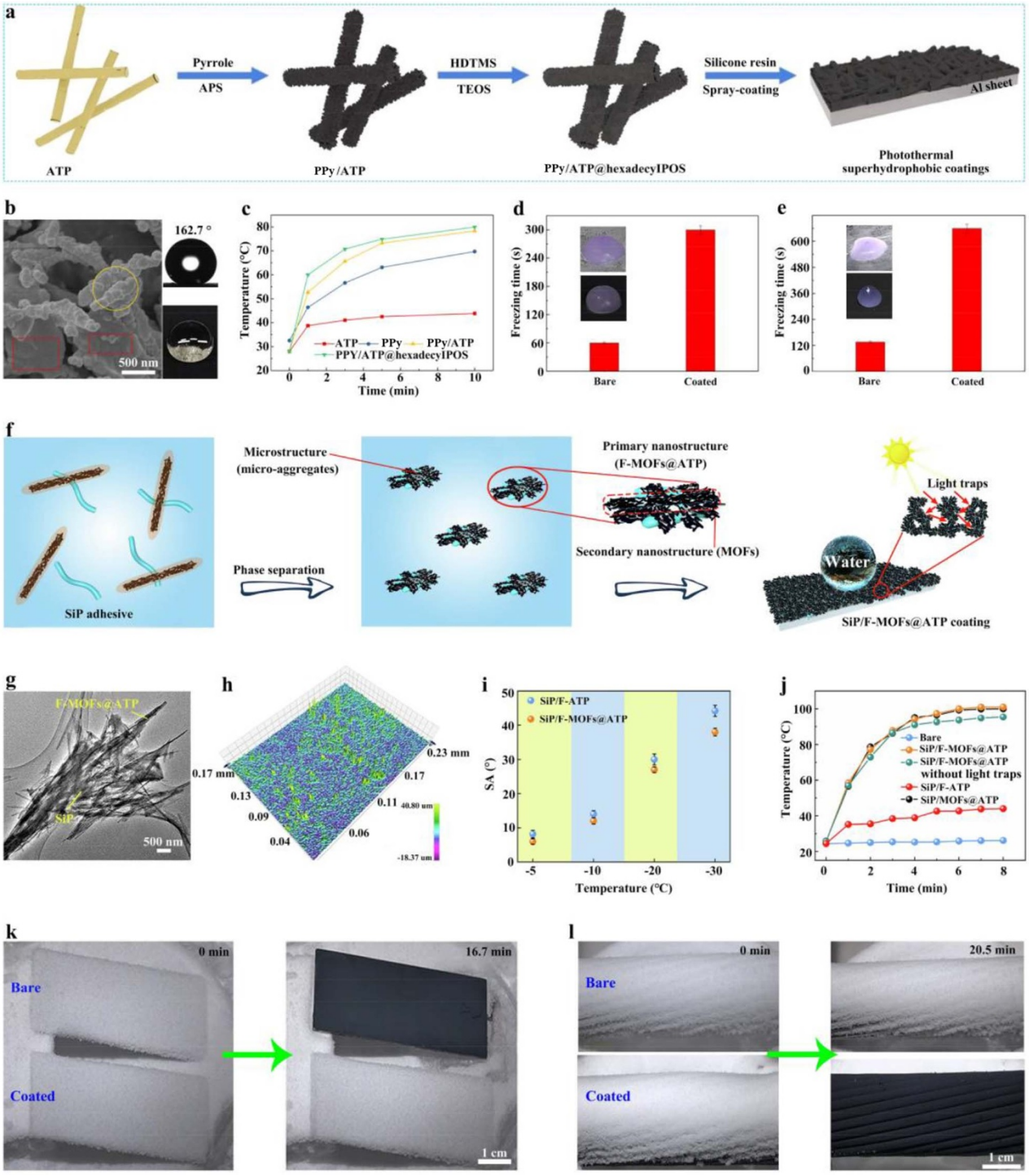


Figure 10. (a) Schematic illustration of the preparation process for PPy/ATP@hexadecylPOS photothermal superhydrophobic coatings. (b) SEM images and water CA of the PPy/ATP@hexadecylPOS coatings, showing a silicone resin-rich phase (red rectangles) and a PPy/ATP@hexadecylPOS-rich phase (yellow circle). (c) Surface temperature evolution of various coatings as a function of irradiation time under 1 sun illumination. (d,e) Water freezing time on bare and PPy/ATP@hexadecylPOS-coated aluminium sheets at –10°C under (d) dark conditions and (e) 1 sun irradiation (Xie *et al*., 2022). (f) Schematic illustration of the preparation process for SiP/F-MOFs@ATP coatings. (g) Transmission electron microscopy image of SiP/F-MOFs@ATP. (h) 3D profilometer image of the SiP/F-MOFs@ATP coating. (i) SA of the coating as a function of temperature after storage at low temperature and 80% relative humidity for 1 h. (j) Surface temperature of bare and coated aluminium alloy plates as a function of time under 1 sun irradiation at 25.4°C and 38% relative humidity. (k,l) De-frosting process on (k) bare and coated aluminium alloy plates and (l) cable lines in a –10°C and 80% relative humidity environment under 0.1 sun irradiation (Mao *et al*., 2024b).

of 1.83 μm (Fig. 10h) and a water CA of 165.6°. The SiP/F-MOFs@ATP coating maintained good superhydrophobicity under low-temperature and high-humidity conditions. Even at –20°C or –30°C with 80% relative humidity for 1 h, the coating remained superhydrophobic, although the SA increased (Fig. 10i). The coating exhibited excellent photothermal performance, reaching 101°C

https://doi.org/10.1180/clm.2026.10054 Published online by Cambridge University Press

within 8 min under 1 sun illumination (25.4°C, 38% relative humidity; Fig. 10j), outperforming most reported photothermal superhydrophobic coatings. The superhydrophobic nature and low thermal conductivity of the coating prolonged the water droplet freezing time from 53 s on bare aluminium to 640 s at −10°C and 80% relative humidity. Under weak light (0.1 sun), the photothermal effect of the MOFs elevated the coating surface temperature from −13.3°C to +6.1°C, causing de-iced water droplets to rapidly roll off under low ice adhesion (36.3 kPa). Furthermore, under identical conditions, the coating enabled complete melting and roll-off of a frost layer (∼0.8 mm) on a 20° inclined surface within 16.7 min, whereas no melting was observed on the control sample even after 60 min (Fig. 10k). The defrosting time for a coated cable was also significantly reduced from >60 min for the bare cable to 20.5 min (Fig. 10l). This coating demonstrates excellent comprehensive performance in both simulated and outdoor environments characterized by low temperature, high humidity and weak light, highlighting the practical application potential of ATP nanorods for constructing high-performance photothermal superhydrophobic anti-icing systems.

From the perspective of anti-icing mechanisms, ATP-based coatings achieve ice prevention and removal primarily through two mechanisms: (1) a passive anti-icing mechanism, leveraging the superhydrophobic micro/nano-structure to prolong droplet freezing time and reduce ice adhesion strength; and (2) an active de-icing mechanism, wherein loaded photothermal materials convert solar energy into thermal energy for rapid ice melting, capable of raising the coating surface temperature above the freezing point even under weak light conditions.

Despite significant progress having been achieved in current research, the practical application of ATP-based anti-icing coatings still faces three major challenges. First, regarding fluorine-free strategies, eliminating fluorine-containing materials while maintaining excellent hydrophobicity remains a key objective. Second, concerning long-term service stability, the mechanisms governing performance retention under complex outdoor conditions (e.g. freeze–thaw cycles, ultraviolet irradiation and mechanical abrasion) require in-depth investigation. Third, with respect to extreme environment adaptability, anti-icing efficacy under more severe conditions (lower temperature, higher humidity and weaker light) needs further enhancement. If future research can effectively synergize material design, structural regulation and long-term service evaluation, ATP-based anti-icing coatings hold promise as an ideal solution for addressing ice accumulation issues under complex climatic conditions.

Conclusions, challenges and perspectives

This review systematically summarizes recent progress in ATP-based multifunctional protective coatings. Starting from the intrinsic structural characteristics of ATP – including its rod-like morphology, channel structure and surface activity – the review discusses how different pretreatment strategies regulate its microstructure, pore characteristics, surface chemistry, dispersibility and compatibility with coating matrices. On this basis, the review further summarizes the multifunctional roles of ATP in coating systems and the corresponding protective mechanisms. ATP can act as: (1) a barrier-phase filler to improve the coating density; (2) a micro/nano-container for loading and releasing active agents; and (3) a structural unit for constructing surface roughness and regulating interfacial properties. According to these roles, the applications of ATP-based coatings in anti-corrosion/self-healing, superhydrophobicity, self-cleaning/anti-smudge, anti-icing and anti-bacterial/anti-fouling systems are discussed. Through these aspects, this review aims to clarify the relationships between ATP pretreatment, coating construction and final functional performance and to provide a reference for the design of high-performance multifunctional protective coatings.

Despite considerable progress having been achieved to date, several key issues still constrain the further development of ATP-based multifunctional coatings:

(1) Insufficient understanding of the structure–property relationship. The relationship between pretreatment conditions and the structural evolution of ATP remains inadequately understood. Variations in channel accessibility, surface active sites, aggregation state and interfacial bonding directly influence barrier capability, active agent loading and release and long-term durability. However, these correlations are still largely described in qualitative terms. A more quantitative understanding of the structure–interface–performance relationship is essential to establishing general design principles.
(2) Limited functional integration. Current functionalization strategies primarily aim to improve dispersion and matrix compatibility or to introduce a single target function, while deeper integration between ATP and coating matrices remains limited. Future modification routes should not only strengthen interfacial stability but also endow ATP with more controllable and programmable functionalities.
(3) Unclear synergistic and competitive relationships among functions. Although multifunctionality has become a major development trend, the synergistic and competitive relationships among different functions remain unclear in many systems. For instance, roughness construction, active agent loading, wettability regulation and mechanical robustness do not necessarily evolve synergistically. Without a clear understanding of these coupling effects, multifunctional integration may increase structural complexity without delivering proportional gains in service performance.

Addressing these challenges will require a paradigm shift from empirical materials design towards a quantitative, mechanism-driven understanding of ATP-based coating systems. Future research should prioritize the development of high-throughput characterization and computational modelling approaches to establish predictive structure–property correlations, as well as the design of smart ATP architectures with stimuli-responsive and self-regulating functionalities. Furthermore, it is critical to recognize that current progress has been largely confined to laboratory-scale demonstrations under idealized conditions. To bridge the gap between fundamental research and industrial practical application, subsequent studies must be strategically aligned with real-world industrial production parameters, including considerations of scalability, process stability, cost-effectiveness and long-term performance under complex operational environments. With such advances, ATP – as an abundant, cost-effective and environmentally compatible nanoclay – holds great promise for enabling next-generation protective coatings with integrated, durable and application-adaptive performance.

CRediT authorship contribution statement. Qiaozhi Miao: Methodology, Writing – original draft, Writing – review & editing. Chaoyu Zhang: Writing – review & editing, Formal analysis, Software. Wenbo Wang, Yue Yin, Mei Wu: Conceptualization, Writing – review & editing, Resources, Supervision.

https://doi.org/10.1180/clm.2026.10054 Published online by Cambridge University Press

Financial support. This research was supported by the following projects: the National Natural Science Foundation of China (52561021; 22468033); the Natural Science Foundation of Inner Mongolia Autonomous Region (2024SHZR1554); the Key R&D and Achievement Transformation Project of Inner Mongolia Autonomous Region (2023YFHH0057); Jiangsu Provincial Key Laboratory of Palygorskite Science and Applied Technology, Huaiyin Institute of Technology (HPK202302); and the Program of Higher-Level Talents of Inner Mongolia University (10000-23112101/017).

Competing interests. The authors declare that they have no known competing financial interests or personal relationships that could have appeared to influence the work reported in this paper.

References

AïtAghzzaf A., Rhouta B., Rocca E. & Khalil A. (2017) Grafted palygorskite as containers of heptanoate for corrosion protection of steel in NaCl medium. *Corrosion Science*, **114**, 88–95.

Ali M. Han E.H., Shi H.W. & Iqbal S. (2024) A bi-functional self-healing epoxy composite coating based on coordinated functionalized attapulgite/graphene oxide. *Surface Science*, **677**, 161015.

Ali M., Shi H.W., Jan F., Ahmed S., Song Y.W. & Han E.H. (2025a) A bifunctional self-healing coating enhanced by attapulgite functionalized MXene with inhibitor integration. *Progress in Organic Coatings*, **199**, 108936.

Ali M., Shi H.W., Wu B., Jan F., Ahmed S., Ullah N. *et al.* (2025b) Hydrophobic and self-healing anti-corrosion coatings based on hybrid attapulgite-Ce-MOF pigment. *Progress in Organic Coatings*, **204**, 109281.

Ali M., Shi H.W. & Jan F. (2026) Self-healing epoxy coatings reinforced by attapulgite loaded with a triazole-thiol inhibitor for corrosion protection. *Progress in Organic Coatings*, **214**, 110038.

Barrer R.M. & Mackenzie N. (1954) Sorption by attapulgite. I. Availability of intracrystalline channels. *The Journal of Physical Chemistry*, **58**, 560–568.

Barrios M.S., González L.F., Rodríguez M.V. & Pozas J.M. (1995) Acid activation of a palygorskite with HCl: development of physico-chemical, textural and surface properties. *Applied Clay Science*, **10**, 247–258.

Barthwal S., Jeon Y. & Lim S.H. (2022) Superhydrophobic sponge decorated with hydrophobic MOF-5 nanocoating for efficient oil–water separation and antibacterial applications. *Sustainable Materials and Technologies*, **33**, 00492.

Belaroui L.S., Dali Youcef L., Ouali A., Bengueddach A. & Lopez Galind A. (2014) Mineralogical and chemical characterization of palygorskite from East-Algeria. *Macla: Revista de la Sociedad Española de Mineralogía*, **19**, 1–2.

Beryl J.R. & Xavier J.R. (2023) Halloysite for clay-polymer nanocomposites: effects of nanofillers on the anti-corrosion, mechanical, microstructure, and flame-retardant properties – a review. *Journal of Materials Science*, **58**, 10943–10974.

Best T. & Gelling V.J. (2023) An industrial perspective on challenges in the lifetime prediction of organic coatings: a century retrospective review. *Corrosion*, **79**, 304–327.

Biswas B., Sarkar B. & Naidu R. (2016) Influence of thermally modified palygorskite on the viability of polycyclic aromatic hydrocarbon-degrading bacteria. *Applied Clay Science*, **134**, 153–160.

Biswas B., Grathoff G., Naidu R. & Warr L.N. (2024) The multidisciplinary science of applied clay research: a 2021–2023 bibliographic analysis. *Applied Clay Science*, **258**, 107471.

Boudriche L., Calvet R., Hamdi B. & Balard H. (2011) Effect of acid treatment on surface properties evolution of attapulgite clay: an application of inverse gas chromatography. *Colloids and Surfaces A: Physicochemical and Engineering Aspects*, **392**, 45–54.

Boudriche L., Calvet R., Hamdi B. & Balard H. (2012) Surface properties evolution of attapulgite by IGC analysis as a function of thermal treatment. *Colloids and Surfaces A: Physicochemical and Engineering Aspects*, **399**, 1–10.

Bradley W.F. (1940) The structural scheme of attapulgite. *American Mineralogist: Journal of Earth and Planetary Materials*, **25**, 405–410.

Butt A.M., Wang Y.P., Ma H.T. & Li H.J. (2023) The preparation of cerium nitrate and attapulgite based superhydrophobic epoxy coatings for the corrosion protection of Q355 mild steel surface. *Surface and Coatings Technology*, **473**, 129977.

Cai X., Zhang J.L., Ouyang Y., Ma D., Tan S.Z. & Peng Y.L. (2013) Bacteria-adsorbed palygorskite stabilizes the quaternary phosphonium salt with specific-targeting capability, long-term antibacterial activity, and lower cytotoxicity. *Langmuir*, **29**, 5279–5285.

Cai Y.F., Xue J.Y. & Polya D.A. (2007) A Fourier transform infrared spectroscopic study of Mg-rich, Mg-poor and acid leached palygorskites. *Spectrochimica Acta Part A: Molecular and Biomolecular Spectroscopy*, **66**, 282–288.

Cai Y.F., Yin Y., Zhang Y.L., Yang F.Y., Zhang C.Y. & Wang W.B. (2025) Nanoclay-enabled advanced metal protection: emerging barrier engineering and smart corrosion inhibition strategies. *Coordination Chemistry Reviews*, **545**, 217014.

Cao L.L., Jones A.K., Sikka V.K., Wu J.Z. & Gao D. (2009) Anti-icing superhydrophobic coatings. *Langmuir*, **25**, 12444–12448.

Chang C.H., Hsu M.H., Weng C.J., Hung W.I., Chuang T.L., Chang K.C. *et al.* (2013) 3D-bioprinting approach to fabricate superhydrophobic epoxy/organophilic clay as an advanced anticorrosive coating with the synergistic effect of superhydrophobicity and gas barrier properties. *Journal of Materials Chemistry A*, **1**, 13869–13877.

Chen D., Zhang J., Zhai M., Chen X., Miao L., Li K. *et al.* (2025) Rational reconstruction from attapulgite to MCM-41 and its superior application in formaldehyde degradation. *Catalysis Science & Technology*, **15**, 2186–2201.

Cheng H.F, Yang J. & Frost R.L. (2011) Thermogravimetric analysis-mass spectrometry (TG-MS) of selected Chinese palygorskites – implications for structural water. *Thermochimica Acta*, **512**, 202–207.

Ci X., Zhao W. & Gao W. (2022) Achieving high loading inhibitor carriers with pH-response for active corrosion protection using attapulgite. *Materials Today Nano*, **19**, 100228.

Cong Q., Qin X.Z., Chen T.K., Jin J.F., Liu C.Z. & Wang M.Q. (2023) Research progress of superhydrophobic materials in the field of anti-/de-icing and their preparation: a review. *Materials*, **16**, 5151.

Ding J.J., Huang D.J., Wang W.B., Wang Q. & Wang A.Q. (2019). Effect of removing coloring metal ions from the natural brick-red palygorskite on properties of alginate/palygorskite nanocomposite film. *International Journal of Biological Macromolecules*, **122**, 684–694.

Ding J.J., Zhang H., Wang W.B., Zhu Y.F., Wang Q. & Wang A.Q. (2021) Synergistic effect of palygorskite nanorods and ion crosslinking to enhance sodium alginate-based hydrogels. *European Polymer Journal*, **147**, 110306.

Dong J., Ding W., Wei J.F., Tian N., Nan X.L. & Zhang J.P. (2023) Preparation of food grade superhydrophobic coatings based on attapulgite nanorods. *ACS Sustainable Chemistry & Engineering*, **11**, 1405–1413.

Dong S.T., Li B.C., Zhang J.P. & Wang A.Q. (2018) Superamphiphobic coatings with low sliding angles from attapulgite/carbon composites. *Advanced Materials Interfaces*, **5**, 1701520.

España V.A.A., Sarkar B., Biswas B., Rusmin R. & Naidu R. (2019) Environmental applications of thermally modified and acid activated clay minerals: current status of the art. *Environmental Technology & Innovation*, **13**, 383–397.

Farhadi S., Farzaneh M. & Kulinich S.A. (2011) Anti-icing performance of superhydrophobic surfaces. *Applied Surface Science*, **257**, 6264–6269.

Feng F., Zhang X., Mu B., Wang P.X., Chen Z.S., Zhang J.H. *et al.* (2022) Attapulgite doped with Fe and Cu nanooxides as peroxidase nanozymes for antibacterial coatings. *ACS Applied Nano Materials*, **5**, 16720–16730.

Frini S.N. & Srasra E. (2010) Acid treatment of south Tunisian palygorskite: removal of Cd(II) from aqueous and phosphoric acid solutions. *Desalination*, **250**, 26–34.

Frini-Srasra N. & Srasra E. (2008) Effect of heating on palygorskite and acid treated palygorskite properties. *Surface Engineering and Applied Electrochemistry*, **44**, 43–49.

Galán E., Mesa J.M. & Sánchez C. (1994) Properties and applications of palygorskite clays from Ciudad Real, central Spain. *Applied Clay Science*, **9**, 293–302.

Galán E. (1996) Properties and applications of palygorskite–sepiolite clays. *Clay Minerals*, **31**, 443–453.

Gao S.T., Shi H.W., Ali M. & Hao L. (2025) Enhanced active protection of epoxy coatings utilizing attapulgite–tannic acid hybrid pigment on carbon steel. *Materials Today Communications*, **46**, 112606.

https://doi.org/10.1180/clm.2026.10054 Published online by Cambridge University Press

Gao W.T., Mu B., Yang F.F., Li Y.L. & Wang A.Q. (2024) Green preparation of licorice flavonoids/ZnO/attapulgite nanocomposites for multifunctional chitosan-based food packaging films. *LWT*, **201**, 116273.

García-Rivas J., Sánchez del Río M., García-Romero E. & Suárez M. (2017) An insight in the structure of a palygorskite from Palygorskaja: some questions on the standard model. *Applied Clay Science*, **148**, 39–47.

Gonzalez F., Pesquera C., Benito I., Mendioroz S. & Pajares J.A. (1989) Mechanism of acid activation of magnesic palygorskite. *Clays and Clay Minerals*, **37**, 258–262.

Guan Y., Wang S.M., Wang X., Sun C., Wang Y.B. & Hu L.J. (2018) Preparation of mesoporous Al-MCM-41 from natural palygorskite and its adsorption performance for hazardous aniline dye-basic fuchsin. *Microporous and Mesoporous Materials*, **265**, 266–274.

Guo X.D., Guo R.B., Fang M.Q., Wang N., Liu W.T., Pei H.B. *et al.* (2022) A novel composite protective coating with UV and corrosion resistance: load floating and self-cleaning performance. *Ceramics International*, **48**, 17308–17318.

He D.T., Han H.C., Yi M., Xu Z.J, Hui H.J., Wang R.F. & Zhou M. (2025) Overview of smart anti-corrosion coatings and their micro/nanocontainer gatekeepers. *Materials Today Communications*, **42**, 111316.

He T.F. & Jin B.S. (2023) Alkali-modified halloysite for enhanced cadmium/lead vapor capture: focus on silicic surface *via* experimental and computational investigations. *Chemical Engineering Journal*, **475**, 145726.

Hizal F., Rungraeng N., Lee J., Jun S., Busscher H.J., van der Mei H.C. & Choi C.H. (2017) Nanoengineered superhydrophobic surfaces of aluminum with extremely low bacterial adhesivity. *ACS Applied Materials & Interfaces*, **9**, 12118–12129.

Hooda A., Goyat M.S., Pandey J.K., Kumar A. & Gupta R. (2020) A review on fundamentals, constraints and fabrication techniques of superhydrophobic coatings. *Progress in Organic Coatings*, **142**, 105557.

Huo C.L. & Yang H.M. (2010) Synthesis and characterization of ZnO/palygorskite. *Applied Clay Science*, **50**, 362–366.

Jiang G., Chen L., Zhang S.D. & Huang H.X. (2018) Superhydrophobic SiC/CNTs coatings with photothermal deicing and passive anti-icing properties. *ACS Applied Materials & Interfaces*, **10**, 36505–36511.

Jiang J.L., Chen Z.G., Duanmu C.S., Gu Y.X., Chen J. & Ni L.N. (2014) Economical synthesis of amorphous carbon nanotubes and SBA-15 mesoporous materials using palygorskite as a template and silica source. *Materials Letters*, **132**, 425–427.

Jiang Y.X., Geng H.L., Peng J.W., Ni X.X., Pei L.C., Ye P. *et al.* (2024) A multifunctional superhydrophobic coating with efficient anti-adhesion and synergistic antibacterial properties. *Progress in Organic Coatings*, **186**, 108028.

Jing Y.M., Mu B., Zhang M.M., Wang L., Zhong H.Q., Liu X.Y. & Wang A.Q. (2020) Zinc-loaded palygorskite nanocomposites for catheter coating with excellent antibacterial and anti-biofilm properties. *Colloids and Surfaces A: Physicochemical and Engineering Aspects*, **600**, 124965.

Kreder M.J., Alvarenga J., Kim P. & Aizenberg J. (2016) Design of anti-icing surfaces: smooth, textured or slippery? *Nature Reviews Materials*, **1**, 15003.

Kuang W.X., Glenn A.F. & Detellier C. (2004) Dehydration and rehydration of palygorskite and the influence of water on the nanopores. *Clays and Clay Minerals*, **52**, 635–642.

Leal D.A., Kuznetsova A., Silva G.M., Tedim J., Wypych F. & Marino C.E.B. (2022) Layered materials as nanocontainers for active corrosion protection: a brief review. *Applied Clay Science*, **225**, 106537.

Lei H., Wei Q.N., Wang Q., Su A.X., Xue M., Li Q. & Hu Q.H. (2017) Characterization of ginger essential oil/palygorskite composite (GEO-PGS) and its anti-bacteria activity. *Materials Science and Engineering: C*, **73**, 381–387.

Li B.C., Liang W.D., Zhang B.B. & Zhang J.P. (2023) Waterborne robust superamphiphobic coatings based on palygorskite for self-cleaning and anti-fouling. *Colloids and Surfaces A: Physicochemical and Engineering Aspects*, **672**, 131759.

Li J., Yin Y., Meng L.J., Qiao H., Zhang H., Cai Y.F. *et al.* (2025) Green porous attapulgite containers enhance the corrosion protection of smart coating. *Progress in Organic Coatings*, **205**, 109285.

Li X., Wu B., Chen H., Nan K.H., Jin Y.Y., Sun L. & Wang B.L. (2018) Recent developments in smart antibacterial surfaces to inhibit biofilm formation and bacterial infections. *Journal of Materials Chemistry B*, **6**, 4274–4292.

Li X.G., Zhang D.W., Liu Z.Y., Li Z., Du C.W. & Dong C.F. (2015) Materials science: share corrosion data. *Nature*, **527**, 441–442.

Li X.Y., Jiang Y., Liu X.Q., Shi L.Y., Zhang D.Y. & Sun L.B. (2017) Direct synthesis of zeolites from a natural clay, attapulgite. *ACS Sustainable Chemistry & Engineering*, **5**, 6124–6130.

Li Y.F. & Nan F. (2023) Achieving long term anti-corrosion waterborne epoxy coating by attapulgite loaded octadecylamine/graphene nanocomposite. *Polymer Testing*, **129**, 108290.

Lisuzzo L., Bertini M., Lazzara G., Ferlito C., Ferrante F. & Duca D. (2023) A computational and experimental investigation of the anchoring of organosilanes on the halloysite silicic surface. *Applied Clay Science*, **245**, 107121.

Liu H.B., Chen T.H., Chang D.Y., Cheng S.Q., Kong D.J., Chen D. *et al.* (2013) Effect of rehydration on structure and surface properties of thermally treated palygorskite. *Journal of Colloid and Interface Science*, **393**, 87–91.

Liu J., He T.L., Zhang H., Tian X.G., Liu H., Zhu J. *et al.* (2025) CuTA/APT@APGQAS/B72 nanocomposite protective coatings: adapting to life in an outdoor mural environment. *Journal of Cultural Heritage*, **71**, 431–439.

Liu X., Zhan T.R. & Zhang B.B. (2024) Attapulgite-based superhydrophobic coating on aluminum alloy substrate with self-cleaning, anti-corrosion and robustness. *Journal of Industrial and Engineering Chemistry*, **130**, 357–367.

Liu X.H., Cheng Y.C., Wang W., Liu F.H. & Hou B.R. (2018a) Application of 1D attapulgite as reservoir with benzotriazole for corrosion protection of carbon steel. *Materials Chemistry and Physics*, **205**, 292–302.

Liu X.H., Zhang D.W., Hou P.M., Pan J., Zhao X. & Hou B.R. (2018b) Preparation and characterization of polyelectrolyte-modified attapulgite as nanocontainers for protection of carbon steel. *Journal of The Electrochemical Society*, **165**, 907–915.

Liu X.H., Wang N. & Hou B.R. (2021) Multifunctional Ag-based ternary nanocomposite incorporated epoxy coating as antibacterial, anticorrosion and antifouling agent. *Corrosion Engineering, Science and Technology*, **56**, 144–153.

Long Y. F., Yin X.X., Mu P., Wang Q.T., Hu J.J. & Li J. (2020) Slippery liquid-infused porous surface (SLIPS) with superior liquid repellency, anti-corrosion, anti-icing and intensified durability for protecting substrates. *Chemical Engineering Journal*, **401**, 126137.

Lu H., Shen H., Song Z., Shing K.S., Tao W. & Nutt S. (2005) Rod-like silicate–epoxy nanocomposites. *Macromolecular Rapid Communications*, **26**, 1445–1450.

Lu Y.S. & Wang A.Q. (2022) From structure evolution of palygorskite to functional material: a review. *Microporous and Mesoporous Materials*, **333**, 111765.

Lv J.Y., Song Y.L., Jiang L. & Wang J.J. (2014) Bio-inspired strategies for anti-icing. *ACS Nano*, **8**, 3152–3169.

Ma M. & Hill R.M. (2006) Superhydrophobic surfaces. *Current Opinion in Colloid & Interface Science*, **11**, 193–202.

Mao J.S., Hong W., Li Q., Gao Y., Jiang Y., Li Y.W. *et al.* (2024a) The application strategies and progresses of silicon-based minerals in advanced oxidation processes for water decontamination. *Coordination Chemistry Reviews*, **511**, 215871.

Mao M.Y., Wei J.F., Li B.C., Li L.X., Huang X.P. & Zhang J.P. (2024b) Scalable robust photothermal superhydrophobic coatings for efficient anti-icing and de-icing in simulated/real environments. *Nature Communications*, **15**, 9610.

Meng J.Q., Wang J., Wang L.J., Lyu C.H., Chen H.Y., Lyu Y.P. & Nie B.S. (2024) Preparation and performance of superhydrophobic surfaces with low surface energy modified attapulgite. *Journal of Molecular Structure*, **1295**, 136586.

Montemor M.F. (2014) Functional and smart coatings for corrosion protection: a review of recent advances. *Surface and Coatings Technology*, **258**, 17–37.

Mu B., Kang Y.R. & Wang A.Q. (2013a) Preparation of a polyelectrolyte-coated magnetic attapulgite composite for the adsorption of precious metals. *Journal of Materials Chemistry A*, **1**, 4804–4811.

Mu B., Wang Q. & Wang A.Q. (2013b) Preparation of magnetic attapulgite nanocomposite for the adsorption of Ag^{+} and application for catalytic reduction of 4-nitrophenol. *Journal of Materials Chemistry A*, **1**, 7083–7090.

Murray H.H. (2000) Traditional and new applications for kaolin, smectite, and palygorskite: a general overview. *Applied Clay Science*, **17**, 207–221.

https://doi.org/10.1180/clm.2026.10054 Published online by Cambridge University Press

Myriam M., Suarez M. & Martin-Pozas J.M. (1998) Structural and textural modifications of palygorskite and sepiolite under acid treatment. *Clays and Clay Minerals*, **46**, 225–231.

Naciri Y., Ghazzal M.N. & Paineau E. (2024) Nanosized tubular clay minerals as inorganic nanoreactors for energy and environmental applications: a review to fill current knowledge gaps. *Advances in Colloid and Interface Science*, **326**, 103139.

Nan F., Liu C.B. & Pu J.B. (2019) Anticorrosive performance of waterborne epoxy coatings containing attapulgite/graphene nanocomposites. *Surface Topography: Metrology and Properties*, **7**, 024002.

Navarchian A.H., Joulazadeh M. & Karimi F. (2014) Investigation of corrosion protection performance of epoxy coatings modified by polyaniline/clay nanocomposites on steel surfaces. *Progress in Organic Coatings*, **77**, 347–353.

Ni L.L., Li S.S., Liu Y.T., Jiang X.W., Cai P., Feng L.D. *et al.* (2021) Fabrication of active corrosion protection waterborne polyurethane coatings using cerium modified palygorskite nanocontainers. *Journal of Applied Polymer Science*, **138**, 50899.

Post J.E. & Heaney P.J. (2008) Synchrotron powder X-ray diffraction study of the structure and dehydration behavior of palygorskite. *American Mineralogist*, **93**, 667–675.

Qian F., Liu X.H., Cui R., Wang K., Wang C., Bao X. *et al.* (2025) Corrosive study of B10/B30 copper-nickel alloys coupled pipeline in static seawater. *Advanced Composites and Hybrid Materials*, **8**, 113.

Qiu S., Yang B., Zhang N., Zhang H.M., Li H.P. & Chen B.B. (2023) Enhanced durability and self-healing properties of palygorskite-based superhydrophobic coatings. *Colloids and Surfaces A: Physicochemical and Engineering Aspects*, **663**, 130981.

Rao A.V., Latthe S.S., Nadargi D.Y., Hirashima H. & Ganesan V. (2009) Preparation of MTMS based transparent superhydrophobic silica films by sol–gel method. *Journal of Colloid and Interface Science*, **332**, 484–490.

Shawabkeh R.A., Al-Khashman O.A., Al-Omari H.S. & Shawabkeh A.F. (2007) Cobalt and zinc removal from aqueous solution by chemically treated bentonite. *The Environmentalist*, **27**, 357–363.

Si Y.F. & Guo Z.G. (2015) Superhydrophobic nanocoatings: from materials to fabrications and to applications. *Nanoscale*, **7**, 5922–5946.

Suárez M. & García-Romero E. (2011) Advances in the crystal chemistry of sepiolite and palygorskite. *Developments in Clay Science*, **3**, 33–65.

Suárez M., García-Rivas J., Morales J., Lorenzo A., García-Vicente A. & García-Romero E. (2021) Review and new data on the surface properties of palygorskite: a comparative study. *Applied Clay Science*, **215**, 106311.

Tan Y., Yin C.J., Zheng S.L., Di Y.H., Sun Z.M. & Li C.Q. (2021) Design and controllable preparation of Bi_2MoO_6/attapulgite photocatalyst for the removal of tetracycline and formaldehyde. *Applied Clay Science*, **215**, 106319.

Tang Q.G., Yang Y., Wang F., Liang X.H., Zhang F.Q. & Liang J.S. (2014) Effect of acid on surface properties of modified attapulgite and performance of styrene butadiene rubber filled by modified attapulgite. *Nanoscience and Nanotechnology Letters*, **6**, 231–237.

Thomas D., Reshmy R., Philip E., Sindhu R., Ulaet S.B., Pugazhendhi A. & Awasthi M.K. (2022) Developments in smart organic coatings for anti-corrosion applications: a review. *Biomass Conversion and Biorefinery*, **12**, 4683–4699.

Udoh I.I., Ekerenam O.O., Daniel E.F., Ikeuba A.I., Njoku D.I., Kolawole S.K. *et al.* (2024) Developments in anticorrosive organic coatings modulated by nano/microcontainers with porous matrices. *Advances in Colloid and Interface Science*, **330**, 103209.

VanScoyoc G.E., Serna C.J. & Ahlrichs J.L. (1979) Structural changes in palygorskite during dehydration and dehydroxylation. *American Mineralogist*, **64**, 215–223.

Volzone C. (2007) Retention of pollutant gases: comparison between clay minerals and their modified products. *Applied Clay Science*, **36**, 191–196.

Wang C.X., Wang N., Jiang K.Y., Ji W.J., Liu Y.J., Tian F. & Zhang X.F. (2024) A robust and multifunctional superhydrophobic coating based on natural palygorskite for corrosion protection of aluminum alloys. *Surface & Coatings Technology*, **485**, 130930.

Wang C.X., Wang W. & Zhang X.F. (2025a) Mechanically durable PAL-based superhydrophobic composite coatings with a sandwich structure for corrosion protection of aluminum alloys. *Progress in Organic Coatings*, **209**, 109616.

Wang C.X., Wang W., Wang N. & Zhang X.F. (2025b) Durable and multifunctional superhydrophobic composite coating based on activated PAL for active protection of aluminum alloy. *Applied Surface Science*, **716**, 164717.

Wang D.H., Sun Q.Q., Hokkanen M.J., Zhang C.L., Lin F.Y., Liu Q. *et al.* (2020a) Design of robust superhydrophobic surfaces. *Nature*, **582**, 55–59.

Wang J., Yin Y.Y., Jin H.X., Zhang J.W., Li Y., Wang C.W. & Duan M.Y. (2019a) The tightly embedded La_2O_3@TiO_2 composite films with cracked surface and their enhanced electro-wetting performance. *Journal of Alloys and Compounds*, **776**, 560–567.

Wang J., Zhang J.W., Yin Y.Y, Jin H.X., Liu S., Li Y. & Wang C.W. (2019b) The stable superhydrophobic ZnO@stearic acid nanocone array and its remarkable all-sided protective abilities in various extreme environments. *Journal of Alloys and Compounds*, **807**, 151663.

Wang J.W., Liu H.B., Xu Z.H., Zhang Y.B., Wang X.S. & He Q. (2025c) A robust and durable superamphiphobic composite coating for preventing the freezing of oil-containing water droplets. *Applied Surface Science*, **712**, 164169.

Wang K.L., Wang L.J., Zhang Y., Zhang Y.D. & Liang J.S. (2020b) Microstructural evolution and sintering properties of palygorskite nanofibers. *International Journal of Applied Ceramic Technology*, **17**, 1833–1842.

Wang L., Wang F., Huang B. & Tang Q.G. (2020c) Recent advances in superhydrophobic composites based on clay minerals. *Applied Clay Science*, **198**, 105793.

Wang L.Z., Tian Z., Jiang G.C., Luo X., Chen C.H., Hu X.Y. *et al.* (2022) Spontaneous dewetting transitions of droplets during icing & melting cycle. *Nature Communications*, **13**, 378.

Wang Q., Zhang J.P. & Wang A.Q. (2013a) Alkali activation of halloysite for adsorption and release of ofloxacin. *Applied Surface Science*, **287**, 54–61.

Wang R.G., Li Z., Wang Y.M., Liu W.B., Deng L.B., Jiao W.C. & Yang F. (2013b) Effects of modified attapulgite on the properties of attapulgite/epoxy nanocomposites. *Polymer Composites*, **34**, 22–31.

Wang W.B. & Wang A.Q. (2016) Recent progress in dispersion of palygorskite crystal bundles for nanocomposites. *Applied Clay Science*, **119**, 18–30.

Wang W.B., Wang F.F., Kang Y.R. & Wang A.Q. (2013c) Facile self-assembly of Au nanoparticles on a magnetic attapulgite/Fe_3O_4 composite for fast catalytic decoloration of dye. *RSC Advances*, **3**, 11515–11520.

Wang W.B., Wang F.F., Kang Y.R. & Wang A.Q. (2015a) Enhanced adsorptive removal of methylene blue from aqueous solution by alkali-activated palygorskite. *Water, Air, & Soil Pollution*, **226**, 83.

Wang W.B., Zhang Z.F., Tian G.Y. & Wang A.Q. (2015b) From nanorods of palygorskite to nanosheets of smectite *via* a one-step hydrothermal process. *RSC Advances*, **5**, 58107–58115.

Wang Y.S., Liang D.F., Wang Q., Shi L.W., Xu W.Q., Li C. *et al.* (2025d) Optimization of attapulgite acidification temperature in NiCo/attapulgite for dry reforming of methane. *Chemical Engineering Journal*, **520**, 165920.

Wang Y.T., Lian Y.C., Zhang M.X., Zhao S.Y., Li Y.H., Tao S.Y. & Liu W.D. (2026) Robust self-healing superhydrophobic coating for anti-icing. *Journal of Colloid and Interface Science*, **708**, 139836.

Wei H.G., Wang Y.R., Guo J., Shen N.Z., Jiang D.W., Zhang X. *et al.* (2015) Advanced micro/nanocapsules for self-healing smart anticorrosion coatings. *Journal of Materials Chemistry A*, **3**, 469–480.

Wei J.F., Li B.C., Tian N., Zhang J.J., Liang W.D. & Zhang J.J. (2022) Scalable robust superamphiphobic coatings enabled by self-similar structure, protective micro-skeleton, and adhesive for practical anti-icing of high-voltage transmission tower. *Advanced Functional Materials*, **32**, 2206014.

Wei J.F., Zhang J.J., Cao X.J., Huo J.H., Huang X.P. & Zhang J.P. (2023) Durable superhydrophobic coatings for prevention of rain attenuation of 5G/weather radomes. *Nature Communications*, **14**, 2862.

Wu Q.W., Liao J. & Yang H.M. (2023a) Recent advances in kaolinite nanoclay as drug carrier for bioapplications: a review. *Advanced Science*, **10**, 2300672.

Wu Y.H., Wei J.M., Shi X.L. & Zhao W.J. (2023b) Achieving anti-corrosion and anti-biofouling dual-function self-healing coating by natural carrier attapulgite loading with 2-undecylimidazoline. *Journal of Materials Science & Technology*, **148**, 222–234.

Xavier J.R. (2023) Multifunctional nanocomposite coatings for superior anticorrosive, flame retardant and mechanical properties in aerospace components. *Surfaces and Interfaces*, **38**, 102832.

https://doi.org/10.1180/clm.2026.10054 Published online by Cambridge University Press

Xiang G.G., Zheng H.P., Lin B., Wang Y.Y., Zhang H.L., Wang D. *et al.* (2024) Modified basalt material reinforced organic coatings: a review. *Corrosion Communications*, **13**, 37–48.

Xie H., Wei J.F., Duan S.Y., Zhu Q., Yang Y.F., Chen K. *et al.* (2022) Non-fluorinated and durable photothermal superhydrophobic coatings based on attapulgite nanorods for efficient anti-icing and deicing. *Chemical Engineering Journal*, **428**, 132585.

Xie W.M., Chen Y. & Yang H.M. (2023a) Layered clay minerals in cancer therapy: recent progress and prospects. *Small*, **19**, 2300842.

Xie Z.T., Tian Y., Shao Y.C., Wang H., Chen R., Zhu X. & Liao Q. (2023b) Recent progress in anti-icing and deicing applications of the photothermal conversion materials. *Progress in Organic Coatings*, **184**, 107834.

Xu H., Ali M., Wu B., Shi H.W., Gu S.H. & Han, E.H. (2025) Anticorrosive behavior of polyurethane coating containing hybrid attapulgite pigment. *Progress in Organic Coatings*, **200**, 109035.

Xu J.X, Wang W.B. & Wang A.Q. (2013a) Effect of solvents treatment on microstructure and dispersion properties of palygorskite. *Journal of Dispersion Science and Technology*, **34**, 334–341.

Xu J.X, Wang W.B. & Wang A.Q. (2013b) Effects of solvent treatment and high-pressure homogenization process on dispersion properties of palygorskite. *Powder Technology*, **235**, 652–660.

Xue S.Y., Li B.F., Mu P. & Li J. (2022) Designing attapulgite-based self-healing superhydrophobic coatings for efficient corrosion protection of magnesium alloys. *Progress in Organic Coatings*, **170**, 106966.

Yang F.F., Li Y.L., Xu J., Kang Y.R., Mu B. & Wang A.Q. (2024) Reconciling the monodispersity of bioinspired ZnO nanoparticles on palygorskite nanorods for a well-balanced antibacterial effect and biocompatibility. *Ceramics International*, **50**, 35236–35246.

Yang H.M., Deng Y.H., Du C.F. & Jin S.M. (2010) Novel synthesis of ordered mesoporous materials Al-MCM-41 from bentonite. *Applied Clay Science*, **47**, 351–355.

Yang Y.M., Gu X., Qian Y.H., Jiang J.L. & Du W.G. (2011) Preparation and antibacterial property study of Ag/AgBr/TiO_2/palygorskite antibacterial agent. *Non-Metallic Mines*, **34**, 53–55.

Ye H.P., Chen F.Z., Sheng Y.Q., Sheng G.Y. & Fu J.M. (2006) Adsorption of phosphate from aqueous solution onto modified palygorskites. *Separation and Purification Technology*, **50**, 283–290.

Yeh J.M. & Chang K.C. (2008) Polymer/layered silicate nanocomposite anti-corrosive coatings. *Journal of Industrial and Engineering Chemistry*, **14**, 275–291.

Yeh J.T., Wang C.K., Tsai C.C., Lin C.H., Huang C.Y., Chen K.N. *et al.* (2013) Ultradrawing properties of ultra-high molecular weight polyethylene/hydrochloric acid treated attapulgite fibers. *Journal of Polymer Research*, **20**, 240.

Youcef L.D., López-Galindo A., Verdugo-Escamilla C. & Belaroui L.S. (2020) Synthesis and characterization of zeolite LTA by hydrothermal transformation of a natural Algerian palygorskite. *Applied Clay Science*, **193**, 105690.

Yu M.H., Feng J., Yang Q., Dang Z. & Zhang L.J. (2022) Inhibition of organosilane/ATP@HQ self-healing passivator for pyrite oxidation. *Chemosphere*, **287**, 132342.

Yu N.L., Xiao X.Y., Ye Z.H. & Pan G.M. (2018) Facile preparation of durable superhydrophobic coating with self-cleaning property. *Surface and Coatings Technology*, **347**, 199–208.

Zaarei D., Sarabi A.A., Sharif F. & Kassiriha S.M. (2008) Structure, properties and corrosion resistivity of polymeric nanocomposite coatings based on layered silicates. *Journal of Coatings Technology and Research*, **5**, 241–249.

Zahidah K.A., Kakooei S., Ismail M.C. & Raja P.B. (2017) Halloysite nanotubes as nanocontainer for smart coating application: a review. *Progress in Organic Coatings*, **111**, 175–185.

Zhan Y.L., Yu S., Amirfazli A., Rahim Siddiqui A. & Li W. (2022) Recent advances in antibacterial superhydrophobic coatings. *Advanced Engineering Materials*, **24**, 2101053.

Zhang B.B., Liu X., Zhan T.R. & Hou B.R. (2024a) Bilayer coating fabricated on aluminum alloy substrates with superamphiphobicity, corrosion resistance, self-cleaning, and delayed icing properties. *Journal of Materials Research and Technology*, **30**, 8218–8227.

Zhang B.B., Liu X.Z., Wang M. & Hou B.R. (2025a) TiN-loaded photothermal superhydrophobic coating with integrated passive anti-icing, active deicing, and anti-corrosion functions. *Materials Today Physics*, **58**, 101857.

Zhang B.B., Zhang Q.C., Xu W.C. & Hou B.R. (2025b) Facile spray-coated fluorine-free superhydrophobic anti-corrosion and anti-icing coating. *Colloids and Surfaces A: Physicochemical and Engineering Aspects*, **713**, 136515.

Zhang H., Wang W.B., Wang X.W., Xu J., Lu Y.S. & Wang A.Q. (2022) Potential of oxalic acid leached natural palygorskite-rich clay as multidimensional nanofiller to improve polypropylene. *Powder Technology*, **396**, 456–466.

Zhang J.J., Wei J.F., Li B.C., Zhao X. & Zhang J.J. (2021) Long-term corrosion protection for magnesium alloy by two-layer self-healing superamphiphobic coatings based on shape memory polymers and attapulgite. *Journal of Colloid and Interface Science*, **594**, 836–847.

Zhang J.P, Wang Q., Chen H. & Wang A.Q. (2010) XRF and nitrogen adsorption studies of acid-activated palygorskite. *Clay Minerals*, **45**, 145–156.

Zhang P.L., Tian N., Zhang J.P. & Wang A.Q. (2018a) Effects of modification of palygorskite on superamphiphobicity and microstructure of palygorskite@fluorinated polysiloxane superamphiphobic coatings. *Applied Clay Science*, **160**, 144–152.

Zhang Q.C., Liu X., Jiang Y.S. & Zhang B.B. (2024b) Superamphiphobic organosilane-grafted attapulgite as an effective corrosion-resistant and anti-icing coating for aluminum alloy. *Colloids and Surfaces A: Physicochemical and Engineering Aspects*, **696**, 134405.

Zhang R.Q., Qian B.B., Xu K., Said A., Chen K.F., Yang C.L. *et al.* (2025c) Microstructural engineering of two-dimensional clay-based materials for advanced electrochemical energy conversion. *Review of Materials Research*, **1**, 100016.

Zhang Y., Wang W.B., Zhang J.P., Liu P. & Wang A.Q. (2015a) A comparative study about adsorption of natural palygorskite for methylene blue. *Chemical Engineering Journal*, **262**, 390–398.

Zhang Z.F, Wang W.B., Kang Y.R., Zong L. & Wang A.Q. (2015b) Glycine-assisted evolution of palygorskite *via* a one-step hydrothermal process to give an efficient adsorbent for capturing Pb(II) ions. *RSC Advances*, **5**, 96829–96839.

Zhang Z.F., Wang W.B. & Wang A.Q. (2015c) Effects of solvothermal process on the physicochemical and adsorption characteristics of palygorskite. *Applied Clay Science*, **107**, 230–237.

Zhang Z.F., Wang W.B., Kang Y.R., Wang Q. & Wang A.Q. (2018b) Structure evolution of brick-red palygorskite induced by hydroxylammonium chloride. *Powder Technology*, **327**, 246–254.

Zhang Z.F., Wang W.B., Tian G.Y., Wang Q. & Wang A.Q. (2018c) Solvothermal evolution of red palygorskite in dimethyl sulfoxide/water. *Applied Clay Science*, **159**, 16–24.

Zhao D.F., Zhou J. & Liu N. (2006) Preparation and characterization of Mingguang palygorskite supported with silver and copper for antibacterial behavior. *Applied Clay Science*, **33**, 161–170.

Zhong H.Q., Mu B., Zhang M.M., Hui A.P., Kang Y.R. & Wang A.Q. (2020) Preparation of effective carvacrol/attapulgite hybrid antibacterial materials by mechanical milling. *Journal of Porous Materials*, **27**, 843–853.

Zhou Z.Y., Pourhashem S., Wang Z.Q., Duan J.Z., Zhang R.Y. & Hou B.R. (2022) Distinctive roles of graphene oxide, ZnO quantum dots, and their nanohybrids in anti-corrosion and anti-fouling performance of waterborne epoxy coatings. *Chemical Engineering Journal*, **439**, 135765.

Zhuang G.Z., Li L., Li M.Y. & Yuan P. (2022) Influences of micropores and water molecules in the palygorskite structure on the color and stability of Maya blue pigment. *Microporous and Mesoporous Materials*, **330**, 111615.

https://doi.org/10.1180/clm.2026.10054 Published online by Cambridge University Press